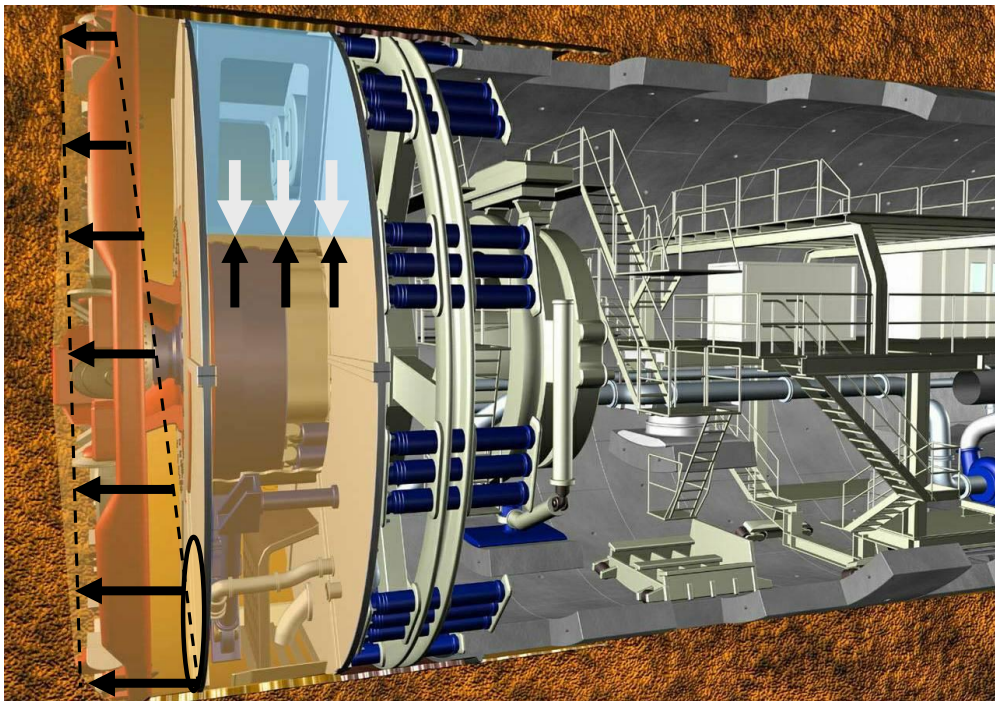


# Recommendations for Face Support Pressure Calculations for Shield Tunnelling in Soft Ground



Deutscher Ausschuss für unterirdisches Bauen e. V.  
German Tunnelling Committee (ITA-AITES)

# Recommendations for Face Support Pressure Calculations for Shield Tunnelling in Soft Ground

Published by:

Deutscher Ausschuss für unterirdisches Bauen e. V. (DAUB)

German Tunnelling Committee (ITA-AITES)

Mathias-Brüggen-Str. 41, 50827 Köln

Tel. +49 - 221 - 5 97 95-0

Fax +49 - 221- 5 97 95-50

E-Mail: [info@daub-ita.de](mailto:info@daub-ita.de)

[www.daub-ita.de](http://www.daub-ita.de)

Prepared by:

Zdenek Zizka and Markus Thewes (Ruhr-University Bochum)

Reviewed by DAUB Working Group Face Support:

Dieter Stephan, Lars Röchter (Ingenieurbüro Vössing)

Christian Späth, Ernst-Rainer Tirpitz, Georg Wicklmayr (Implenia Germany)

Ulrich Maidl, Stefan Hintz (Maidl Tunnelconsultants)

Fritz Grübl (PSP Consulting Engineers)

Rainer Rengshausen (PORR Germany)

Jürgen Schwarz (Bundeswehr University Munich)

Klaus Rieker, Thomas Grubert (Wayss & Freytag)

Ludger Speier (ZPP German Engineering)

Edgar Schömig (Züblin)

October 2016



## Table of contents

List of Variables .....	6
List of Abbreviations.....	9
1 Introduction / Purpose of the document .....	10
2 Tunnel face stability in mechanised tunnelling .....	11
2.1 General conditions for tunnel face stability and the aim of face support pressure calculations .....	11
2.2 Shield machine technology and application ranges .....	11
2.2.1 Shield machines with no face support .....	12
2.2.2 Shield machines with mechanical face support .....	12
2.2.3 Shield machines with compressed-air support .....	12
2.2.4 Shield machines with slurry face support .....	13
2.2.5 Shield machines with earth pressure face support.....	14
2.3 Description of the tunnel face support mechanisms.....	15
2.3.1 Air support.....	15
2.3.2 Earth pressure support (EPB) .....	16
2.3.3 Slurry support.....	16
2.3.4 Support pressure during stoppages and interventions in the excavation chamber .....	16
2.4 Requirements for a particular support medium.....	17
2.4.1 Bentonite slurry.....	17
2.4.2 Earth muck – EPB shield .....	19
3 German safety concept for tunnel face stability .....	22
4 Calculation methods for determination of the required support pressure due to the acting earth pressure .....	24
4.1 Analytical.....	24
4.2 Empirical and experimental methods.....	29
4.3 Numerical.....	31
4.4 Summary .....	32
5 Calculation methods for determination of required support pressure due to the acting water pressure .....	33
6 Face support pressure calculation in practice .....	34
6.1 Limit equilibrium method .....	34
6.2 Stability ratio method .....	42
6.3 Numerical methods .....	46
6.4 Summary .....	46

- 7 Additional aspects to be considered in the analysis ..... 47
  - 7.1 Support pressure deviations ..... 47
  - 7.2 Heterogeneous tunnel face in layered soft ground ..... 47
  - 7.3 Mixed tunnel face with rock and soil ..... 48
  - 7.4 Excess pore pressure during excavation with a slurry shield ..... 49
- 8 Calculation examples ..... 51
  - 8.1 Coarse ground ..... 51
    - 8.1.1 Case 1 – membrane pressure transfer model ..... 51
    - 8.1.2 Case 2 – penetration pressure transfer model ..... 54
  - 8.2 Cohesive ground ..... 57
- 9 References ..... 60
  - 9.1 General references ..... 60
  - 9.2 Websites references ..... 64

## List of Variables

$A$	$[m^2]$	Cross-sectional area of the silo
$AA$	$[m^2]$	Area AA
$BB$	$[m^2]$	Area BB
$b$	$[m]$	Length the silo
$c$	$[kN/m^2]$	Cohesion
$c'_1$	$[kN/m^2]$	Average characteristic cohesion in overburden area
$c'_2$	$[kN/m^2]$	Average characteristic cohesion in tunnel face area
$c_u$	$[kN/m^2]$	Undrained shear strength of the soil
$C$	$[m]$	Depth of cover
$d_{10}$	$[m]$	Characteristic grain size of the soil (to be obtained from grain distribution curve)
$D$	$[m]$	Tunnel diameter
$E_{re}$	$[kN]$	Support force due to earth pressure (rectangular tunnel face)
$E_{max,re}$	$[kN]$	Maximal support force due to earth pressure (rectangular tunnel face)
$E_{max,ci}$	$[kN]$	Maximal support force due to earth pressure (circular tunnel face)
<i>Efficiency</i>	$[kN]$	Efficiency of the pressure transfer
$e_{ah,i}$	$[-]$	Earth pressure of particular lamella
$e_{max}$	$[m]$	Maximal penetration distance of the slurry
$e_{max,a}$	$[m]$	Penetration distance of the slurry tunnel axis
$e_{max,c}$	$[m]$	Penetration distance of the slurry tunnel crown
$e_{max,i}$	$[m]$	Penetration distance of the slurry tunnel invert
$f_{so}$	$[kN/m^3]$	Slurry support pressure gradient
$G$	$[kN]$	Own weight of the wedge
$h$	$[m]$	Height of the failure mechanism, equal to the tunnel diameter within DIN 4085
$h_{w,axis}$	$[m]$	Groundwater level above the tunnel axis
$h_{w,crown}$	$[m]$	Groundwater level above the tunnel crown
$\Delta h$	$[m]$	Thickness of a lamella
$I_c$	$[-]$	Consistency index of a soil
$I_p$	$[-]$	Plasticity limit of a soil
$K_1$	$[-]$	Coefficient of lateral earth pressure in the area of the prism
$K_2$	$[-]$	Coefficient of lateral earth pressure in the area of the wedge
$k$	$[m/s]$	Water permeability of a soil
$k_0$	$[-]$	Coefficient of lateral earth pressure at rest
$k_a$	$[-]$	Rankine's active earth pressure
$k_p$	$[-]$	Rankine's passive earth pressure
$k_{agh,i}$	$[-]$	Active lateral pressure coefficient due to the friction acc. to DIN 4085
$k_{ach,i}$	$[-]$	Active lateral earth pressure coefficient due to the cohesion acc. to DIN 4085
$N$	$[-]$	Stability ratio
$N_{cr}$	$[-]$	Critical stability ratio
$N_{exist}$	$[-]$	Existing stability ratio
$N_s$	$[-]$	Stability factor
$n$	$[-]$	Soil porosity
$P_v$	$[kN]$	Vertical load from the soil prism
$\Delta p$	$[kN/m^2]$	Slurry excess pressure
$\Delta p_c$	$[kN/m^2]$	Slurry excess pressure tunnel crown

$\Delta p_a$	[kN/m <sup>2</sup> ]	Slurry excess pressure tunnel axis
$\Delta p_i$	[kN/m <sup>2</sup> ]	Slurry excess pressure tunnel invert
$Q$	[kN/m <sup>2</sup> ]	Shear force on inclined surface of the wedge
$S_{re}$	[kN]	Required support force (rectangular tunnel face)
$S_{E,ci}$	[kN]	Support force to counter earth pressure considering safety coefficient (circular tunnel face)
$S_{E,trans,ci}$	[kN]	Support force transferred to efficiently counter earth pressure (circular tunnel face)
$S_{ci}$	[kN]	Required support force (circular tunnel face)
$S_{total,trans,ci}$	[kN]	Total support force transferred
$S_{W,ci}$	[kN]	Support force to counter water pressure considering safety coefficient (circular tunnel face)
$S_{axis}$	[kN/m <sup>2</sup> ]	Support pressure in the tunnel axis
$S_{crown}$	[kN/m <sup>2</sup> ]	Support pressure in the tunnel crown
$S_{crown,advance,min}$	[kN/m <sup>2</sup> ]	Minimal support pressure at the tunnel crown for regular advance considering possible support pressure deviations
$S_{crown,advance,max}$	[kN/m <sup>2</sup> ]	Maximal support pressure at the tunnel crown for regular advance considering possible support pressure deviations
$S_{crown,max}$	[kN/m <sup>2</sup> ]	Maximal allowable pressure in the tunnel crown due to break up/ blow out safety
$S_{crown,min}$	[kN/m <sup>2</sup> ]	Minimal support pressure at the tunnel crown to stabilize the tunnel face without consideration of support pressure deviations
$T$	[kN]	Shear resistance force on the vertical triangular plane of the wedge
$T_R$	[kN]	Shear resistance force due to friction
$T_C$	[kN]	Shear resistance force due to cohesion
$t_1$	[m]	Thickness of the soil with drained behaviour above the tunnel crown
$t_2$	[m]	Thickness of the soil with undrained behaviour above the tunnel crown
$t_{axis}$	[m]	Distance from the shield axis to the terrain surface
$t_{crown}$	[m]	Overburden height
$U$	[m]	Circumference length of the silo
$W_{ci}$	[kN]	Support force due to groundwater pressure (circular tunnel face)
$W_{re}$	[kN]	Support force due to groundwater pressure (rectangular tunnel face)
$w_{axis}$	[kN/m <sup>2</sup> ]	Groundwater pressure in the tunnel axis
$w_{crown}$	[kN/m <sup>2</sup> ]	Groundwater pressure at the tunnel crown
$z$	[m]	Vertical coordinate starting from the terrain surface
$z_2$	[m]	Vertical coordinate starting from the tunnel crown
$\Delta$	[kN/m <sup>2</sup> ]	Support pressure deviations
$\Delta_W$	[kN/m <sup>2</sup> ]	Minimal support – overpressure to water pressure
$\gamma$	[kN/m <sup>3</sup> ]	Unit weight of (saturated) soil
$\gamma_1$	[kN/m <sup>3</sup> ]	Soil unit weight in the overburden area
$\gamma'_1$	[kN/m <sup>3</sup> ]	Soil unit weight under buoyancy in the overburden area
$\gamma_{1,av}$	[kN/m <sup>3</sup> ]	Average soil unit weight in the overburden area
$\gamma_{1,av,min}$	[kN/m <sup>3</sup> ]	Minimal Average soil unit weight in the overburden area
$\gamma_2$	[kN/m <sup>3</sup> ]	Soil unit weight in the tunnel face area
$\gamma'_2$	[kN/m <sup>3</sup> ]	Soil unit weight under buoyancy in the tunnel face area
$\gamma_{2,av}$	[kN/m <sup>3</sup> ]	Average soil unit weight in the tunnel face area
$\gamma_{2,sat}$	[kN/m <sup>3</sup> ]	Saturated unit weight of soil 2 with undrained behavior
$\gamma_B$	[kN/m <sup>3</sup> ]	Unit weight of soil grains

$\gamma_F$	[kN/m <sup>3</sup> ]	Unit weight of fresh slurry
$\gamma_G$	[-]	Partial safety factor for permanent load case in GZ1C acc. to DIN 1054 (= 1.00)
$\gamma_i$	[kN/m <sup>3</sup> ]	Unit weight of soil in lamella i
$\gamma_\phi$	[-]	Partial safety coefficient for drained soil within the status GZ1C in load case LF2 acc. to DIN 1054 (= 1.15)
$\gamma_{\phi'}$	[-]	Safety factor for angle of shearing resistance according to EC 7 (Annex A, table A.2)
$\gamma_{c'}$	[-]	Safety factor for effective cohesion according to EC 7 (Annex A, table A.2)
$\gamma_{cu}$	[-]	Safety factor for undrained shear strength according to EC 7 (Annex A, table A.2)
$\gamma_{qu}$	[-]	Safety factor for unconfined strength according to EC 7 (Annex A, table A.2)
$\gamma_\gamma$	[-]	Safety factor for weight density (unit weight) according to EC 7 (Annex A, table A.2)
$\gamma_S$	[kN/m <sup>3</sup> ]	Unit weight of the support medium
$\gamma_w$	[kN/m <sup>3</sup> ]	Unit weight of water
$\delta$	[deg]	Angle of wall friction
$\eta$	[-]	Safety factor
$\eta_E$	[-]	Safety factor for the earth pressure force
$\eta_F$	[-]	Safety factor accounting for deviations in the yield point of suspension
$\eta_w$	[-]	Safety factor for the water pressure force
$\vartheta$	[deg]	Sliding angle
$\vartheta_{crit}$	[deg]	Critical sliding angle
$\mu_{agh}, \mu_{aph}, \mu_{ach}$	[-]	Shape coefficients for earth pressure due to soil friction angle, due to load on the top plane of the failure wedge and due to cohesion acc. to DIN 4085
$\sigma_0$	[kN/m <sup>2</sup> ]	Ground pressure on a retaining wall
$\sigma_s$	[kN/m <sup>2</sup> ]	Surcharge on the surface (Traffic load on the surface)
$\sigma_v(z)$	[kN/m <sup>2</sup> ]	Vertical stress at the elevation z
$\sigma_{v,axis}$	[kN/m <sup>2</sup> ]	Total vertical stress from the overburden at the tunnel axis
$\sigma_{v,crown}$	[kN/m <sup>2</sup> ]	Total vertical stress in the tunnel crown
$\sigma_{v,crown,min}$	[kN/m <sup>2</sup> ]	Total vertical stress in the tunnel crown considering minimal unit weight of soil
$\sigma_{v,interface}$	[kN/m <sup>2</sup> ]	Total stress at the interface between soil 1 (drained) and soil 2 (undrained)
$\tau_f$	[kN/m <sup>2</sup> ]	Yield point of the slurry
$\phi'$	[deg]	Characteristic drained friction angle of the soil
$\phi'_1$	[deg]	Average characteristic drained friction angle of the soil in the overburden
$\phi'_2$	[deg]	Average characteristic drained friction angle of the soil at the tunnel face

## List of Abbreviations

DAUB	Deutscher Ausschuss für Unterirdisches Bauen (German Tunnelling Committee)
DIN	Deutsches Institut für Normung (German Institute for Standardisation)
EC	Eurocode - European standard
EPB	Earth-pressure-balance
FE	Finite Elements
FEM	Finite Element Method
ITA	International Tunnelling and Underground Space Association
NTC	Norme Tecniche per le Costruzioni (Italian design code)
ÖGG	Österreichische Gesellschaft für Geomechanik (Austrian Society for Geomechanics)
RiL	Richtlinie der Deutschen Bahn AG (Standard of German Railways)
WG	Working group of ITA
ZTV-ING	Zusätzliche Technische Vertragsbedingungen und Richtlinien für Ingenieurbauten (Additional terms and conditions and guidelines for engineering structures issued by Bundesanstalt für Straßenwesen, Germany)

## 1 Introduction / Purpose of the document

This document aims to offer a guide to the methods for tunnel face stability assessment in mechanized tunnelling and to provide a best practice guideline for face support pressure calculations. Furthermore, the document intends to help with the choice between available calculation methods depending on the expected ground conditions.

This document consists of seven chapters in total, excluding introduction. The second chapter introduces the general aim of a tunnel face stability assessment and briefly describes soft ground mechanized tunnelling technology with a focus on the tunnel face stability. The German safety concept regarding the face stability assessment is outlined in the third chapter. Following this, the most important scientific approaches dealing with face stability calculations are discussed, in chapter 4 focusing on support pressure due to earth pressure at the tunnel face and in chapter 5 summarizing support pressure due to groundwater pressure. The most relevant calculation methods for shield tunnelling practice are presented in detail in chapter 6. Additional aspects regarding face stability are discussed in chapter 7. Two examples of face support pressure calculations are provided at the end of this document in chapter 8.

This document is intended to be applied to mechanized tunnelling projects in soft ground; hence, the document neither covers the face stability assessment of tunnels in any type of intact or fractured rock nor conventionally excavated tunnels. Due to the variability of ground conditions, this document should not be taken as a strict guideline of required calculations, methodologies and safety concepts to be adopted. Experienced engineering judgement is still required on a case to case basis. Moreover, diverse experiences exist regarding the face stability assessment among the international tunnelling community.

## 2 Tunnel face stability in mechanised tunnelling

### 2.1 General conditions for tunnel face stability and the aim of face support pressure calculations

The aim of tunnel face stability assessment is to investigate groundwater pressure and earth pressure acting at the tunnel face and to analyse the bearing capacity of the tunnel face. If the self-bearing capacity of the tunnel face is insufficient, a tunnel face support has to be provided. In this case, the support medium must counter the earth and groundwater pressures to stabilize the tunnel face.

Two fundamental viewpoints are utilized for tunnel face support design. For the first viewpoint, the tunnel face pressure calculations are dealing solely with tunnel face stability, as presented mostly within this document. The calculations do not consider the development of ground deformations when the calculated support pressure is applied to the tunnel face. This approach is called “the Ultimate Limit State Approach” since only a minimal required face support pressure is determined to avoid a tunnel face collapse. Various analytical calculation methods (see chapter 4) can be employed when adopting the Ultimate Limit State Approach.

The second point of view focuses on keeping the ground deformation below a pre-determined limit. Thus this method defines the support pressure (and consequently the Tail Void Grouting pressure) based on the required ground deformation limit. This approach may be viewed as “the Serviceability Limit State Approach” since it considers ground deformation during excavation to be the main design criterion. Numerical analysis of machine ground interaction (section 6.3) is necessary to be performed for most cases in order to determine support pressure based on the serviceability criterion.

The design of optimal support pressure involves operational considerations as an unnecessary high support pressure is detrimental for the excavation progress because it may cause increased wear of the shield machine and energy consumption. Furthermore, it results in issues regarding work safety during compressed air interventions. It may be the case, that a higher support pressure does not automatically mean more safety for the excavation due to possible resulting break-ups of the overburden or blow-outs of the support medium. On the other hand, a face pressure above the minimum required level may contribute to a reduction of settlement. Lastly, not only is the support pressure level important for a smooth excavation progress, but also the proper selection of a face support type, such as earth-pressure-balance support or slurry support, which predetermines the success of the project even more significantly.

### 2.2 Shield machine technology and application ranges

The type of tunnel face support is of particular importance for mechanized tunnelling in soft ground. Therefore, the DAUB Recommendations for selecting and evaluating Tunnel Boring Machines [DAUB, 2010] classify soft-ground shield machines based on types of tunnel face support (Fig. 1).

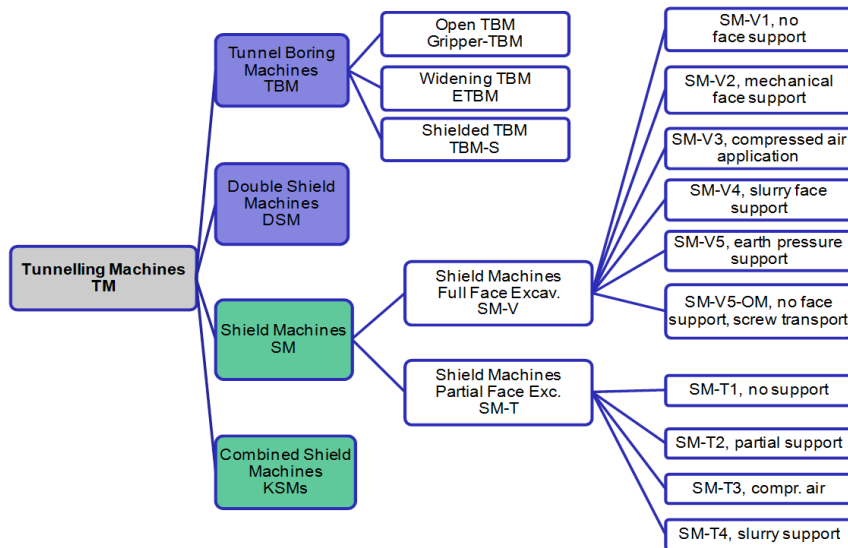


Fig. 1: Classification of tunneling machines after DAUB (2010)

The DAUB Recommendations define five categories of face support mechanisms for shield machines with full face excavation. All available support techniques are presented in this chapter, however particular focus is given to fluid (slurry) supported and earth supported tunnel faces (EPB). This is due to the current amount of shield machine types produced worldwide (Fig. 2).

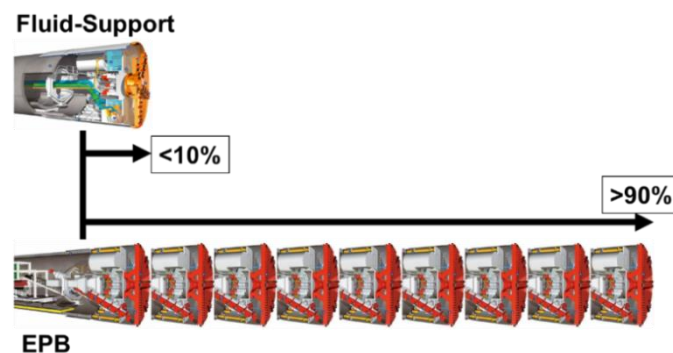


Fig. 2: Approximate comparison of the quantity of different face support machine types that are produced [Thewes, 2007].

### 2.2.1 Shield machines with no face support

The shield machines with “no face support” are described as open shields. The excavation chamber of the machine is at atmospheric pressure. The amount of the soil cut is in balance with the soil discharged from the excavation chamber. This shield can be used when the tunnel face is stable and has no expected groundwater flow towards the face.

### 2.2.2 Shield machines with mechanical face support

Shield machines with mechanical face support were historically used in tunneling. The usage of these machines is no longer recommended.

### 2.2.3 Shield machines with compressed-air support

The excavation chamber of this shield is pressurized by compressed air. This type of the face support can generally be used only to counteract groundwater pressure, so the tunnel face has to be stable in terms of effective stresses (see section 2.3.1). In regular excavation, compressed – air support has become uncommon within soft soils in the last two decades. Slurry and EPB shield machines are still

equipped with additional compressed-air face support systems to enable hyperbaric interventions at the tunnel face during standstills.

#### 2.2.4 Shield machines with slurry face support

The excavation chamber (front chamber) and working chamber (back chamber) of the slurry shield machine are filled with a slurry (Fig. 3). The slurry is a suspension of water and bentonite particles (bentonite consists mostly of montmorillonite clay minerals) and it is also used in diaphragm wall technology. The excavation chamber is separated from the working chamber by a submerged wall. The flow between the two chambers is ensured by an opening at the bottom of the submerged wall. The excavation chamber is completely filled with bentonite suspension while the suspension level in the working chamber is usually adjusted to be slightly above the machine axis. The support pressure in the excavation chamber is controlled by regulating the pressure of the compressed-air reservoir (also called an air cushion or air bubble) in the pressure chamber. Volume fluctuations in the chamber can easily be compensated without significantly changing the support pressure. The excavated soil is mixed with the suspension and pumped through the suction inlet and slurry discharge pipe to a separation plant at ground level. Fresh or regenerated slurry is continuously supplied into the excavation chamber by a slurry feed pipe. Additionally, the machine is equipped with a sieve grill and stone crusher before the suction inlet in order to reduce the size of cobbles for hydraulic transport by the slurry discharge pipe.

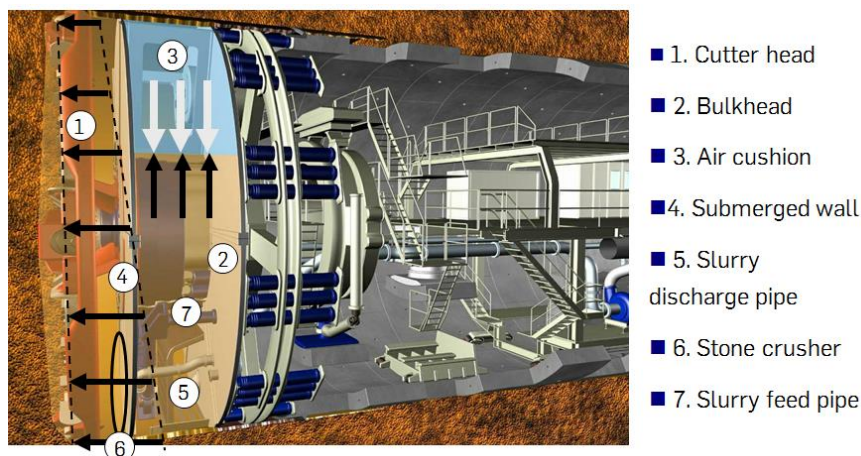


Fig. 3: Slurry shield machine [Herrenknecht.de]

The typical application range of slurry shields is shown in area A (Fig. 4). Grains within this range are small enough to ensure efficient face support by a bentonite suspension but large enough to allow for a simple separation of the spoil. In zone B, which consists of fine-grained soils and clays, the separation effort becomes more difficult, and clogging may occur. Zone C consists of very coarse grained gravels. These types of gravels, especially uniformly graded gravels, have an extremely high permeability. Here, even a highly concentrated bentonite suspension may penetrate into the ground without stagnation, thereby making the face support mechanism inefficient. In this case, fillers should be added to the bentonite suspension to plug the larger pores of ground. Required properties for the bentonite suspension are presented within section 2.4.1.

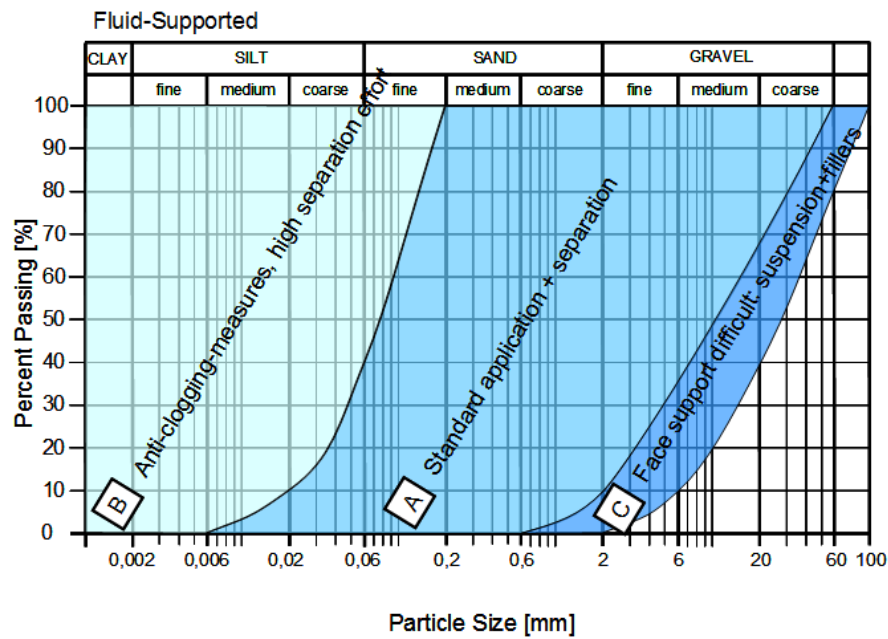


Fig. 4: Application ranges of shield machine with slurry supported tunnel face [Thewes, 2009]

2.2.5 Shield machines with earth pressure face support

Earth Pressure Balanced (EPB) shields (Fig. 5) make use of the excavated ground to provide face support. The soil is excavated by the cutting wheel and enters the excavation chamber. The volume flow of entering soil can be regulated through the excavation speed of the shield machine. The support pressure is regulated by the extraction flow of the screw conveyer and in addition also by the injection of foam for conditioning. The spoil within the excavation chamber must have certain properties in order to provide efficient face support (see section 2.4.2). Spoil properties can be adjusted by mixing with suitable additives, such as foam.

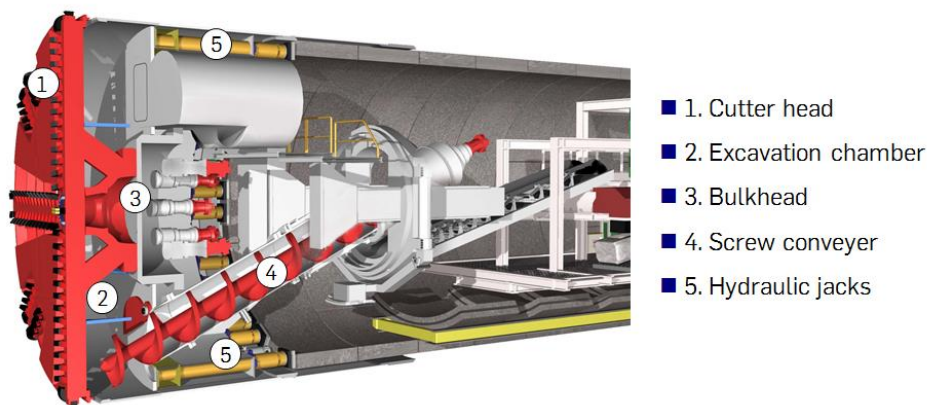


Fig. 5: Earth pressure balanced shield machine (EPB) [Herrenknecht.de]

The primary application range of the EPB shields is in fine-grained soil. The spoil may be conditioned here only by water (Area 1, Fig. 6). Foam has to be injected as a conditioning agent when the excavation is performed through coarser ground (Area 2, Fig. 6). The coarser ground is called the extended application range of the EPB shield. In areas 3 and 4 (Fig. 6), polymers and foam have to be added into the excavation chamber to provide the required properties of the spoil.

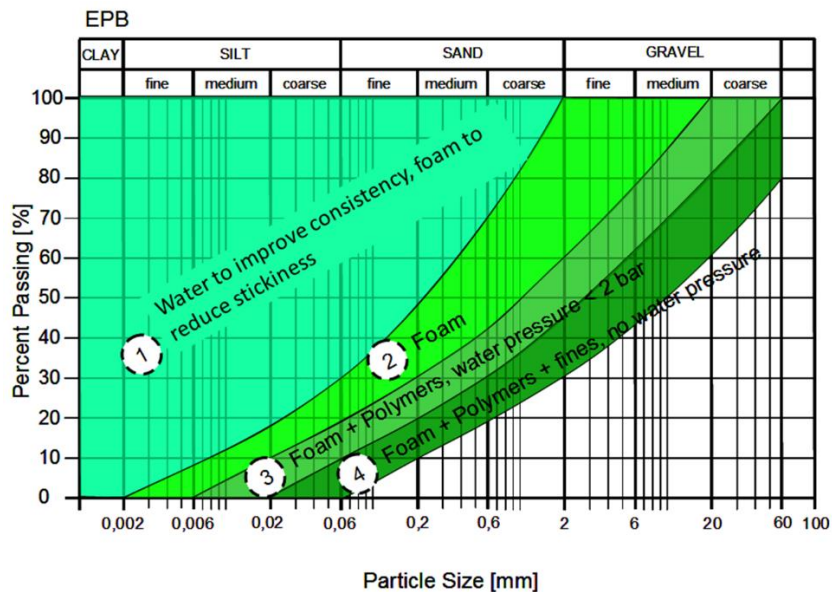


Fig. 6: Application ranges of the EPB shield [Thewes, 2007]

The EPB shield can be operated next to the closed mode described above, in two additional modes depending on the expected stability of the tunnel face [Maidl, 2013]. The three modes are presented in the following:

- **Open mode** – The excavation chamber is almost empty during excavation in open mode. Therefore, no support is provided to the tunnel face. The excavation may be performed in the open mode, if ground conditions assure a completely stable tunnel face, and a possible groundwater flow towards the face or into the excavation chamber does not cause any hydrogeological or shield-operational problems.
- **Transition mode** – The basic feature behind the transition mode is that the EPB shield is operated with a closed but only partially filled excavation chamber. The spoil in the excavation chamber may be pressurized by compressed-air, which helps reduce or avoid groundwater inflow into the excavation chamber. This mode is applicable in cases with a stable tunnel face and low risk of over-excavation at the tunnel face. The main purpose of the transition mode is to control water inflows through the tunnel face. A quick change of this operation mode to the closed mode is possible.
- **Closed mode** – The excavation chamber is completely filled with the excavated soil and is pressurized. The applied pressure balances the acting earth and groundwater pressures. This operation mode is required in unstable soft soils below the groundwater table. Moreover, uncontrolled water inflow can be prevented during excavation when the support pressure is sufficiently high. The support pressure calculation methods introduced in this document are particularly designated to the closed mode.

### 2.3 Description of the tunnel face support mechanisms

This section provides an explanation of the types of face support mechanisms. The “no support” and mechanical support are omitted. The support mechanisms are presented first for the excavation mode and subsequently for shield stoppages and compressed-air interventions.

#### 2.3.1 Air support

Compressed air is present in the excavation chamber. Air enters the pores of the subsoil to balance pore water pressure preventing the occurrence of groundwater flow towards tunnel face. Thus the

effective earth pressure on the tunnel face generally cannot be balanced. This earth pressure may be countered by air pressure only in soil with high capillary forces. CAUTION: During compressed air interventions within slurry or EPB shield tunnelling, another pressure transfer mechanism will be activated.

### 2.3.2 Earth pressure support (EPB)

In EPB, the bulkhead pushes on the spoil in the excavation chamber and the support pressure is transferred to the subsoil in terms of total stress. In the extended application range of EPB shields in non-cohesive soils, this transfer is achieved from lowered permeability of the earth muck in the excavation chamber by soil conditioning. In primary application range in cohesive soils with low permeability, the decrease of permeability is not necessary for pressure transfer due to presence of capillary forces.

### 2.3.3 Slurry support

The interaction between a bentonite suspension and subsoil is crucial for slurry shield driven tunnels. The slurry pressure counters both earth and water pressures in order to stabilize the tunnel face. While the counteraction against water pressure is principally secured, excess slurry pressure must be transferred to the soil skeleton to counteract the earth pressure. Several theories can be found in literature to explain support pressure transfers to soil skeletons (e.g. Müller-Kirchenbauer, 1977; Broere & van Tol, 2000 or Bezuijen et al., 2001). Currently the dominant theory in slurry tunneling practice is taken from diaphragm wall technology (Müller-Kirchenbauer, 1977) and summarized in DIN 4126 (2004). The pressure transfer can be achieved in two ways (Fig. 7), (1) with a membrane or (2) a penetration zone. The membrane (1), also called filter cake, creates a thin impermeable layer directly on the tunnel face, and enables a transformation of excess slurry pressure into effective support stress. In the case of a penetration zone formation (2), the excess slurry pressure is transferred to the soil skeleton along the entire penetration depth by shear stresses between suspension and soil grains.

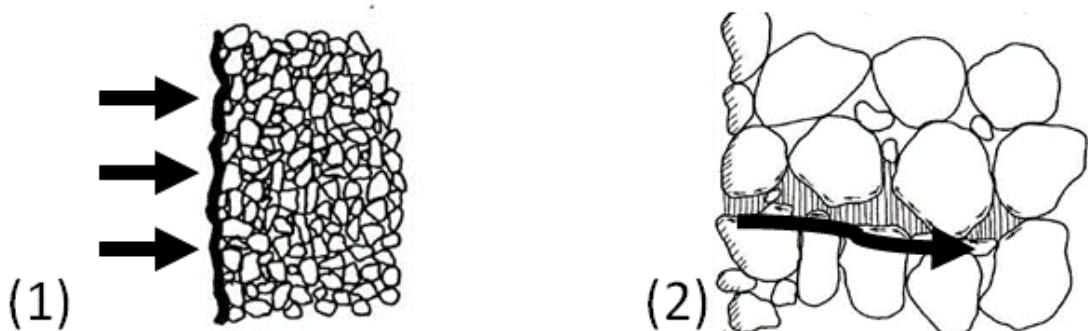


Fig. 7: Slurry excess pressure transfer on the soil skeleton by means of a membrane (1) and a penetration zone (2)

Hence, a general relation exists between the mechanism of pressure transfer and penetration behavior of bentonite suspension into subsoil (Mueller-Kirchenbauer, 1977). On the one hand, the relationship between the size of the bentonite particles in the suspension and the size of the pores in soft soil is decisive. On the other hand, the yield strength of the bentonite suspension is a further determining factor.

### 2.3.4 Support pressure during stoppages and interventions in the excavation chamber

The tunnel face must be supported during all advance modes, not only during the excavation (previously described) but also during stoppages and interventions at the tunnel face.

During stoppages or downtimes, the excavation chamber of an EPB shield usually remains filled. The pressure is maintained by proper injections of foaming agents. Separation of foam and water may cause problems by creating an air bubble at the crown of the excavation chamber. Maintaining tunnel face support during slurry shield downtimes is significantly simpler as the filter cake or penetration zone is already built-up and excess slurry pressure in the excavation chamber is maintained by the mechanism for pressure regulation.

Interventions at the tunnel face are carried out for inspection, and for maintenance work of the cutting wheel. In these cases, the ordinary support medium used during excavation is replaced by compressed-air. The mechanisms of tunnel face support differ slightly depending on the type of machine used. In slurry shield cases, the filter cake on the tunnel face has to be maintained, and eventually renewed during long interventions. The existing filter cake seals the tunnel face and assures the transfer of excess air pressure to the soil skeleton. The renewing of the filter cake is required because it may dry out and shrink during longer interventions. When the filter cake dries out, only reduced excess air pressure can be transferred to the soil skeleton.

In the case of an EPB shield, the difficulty of a compressed-air intervention is dependent on the present ground type on the tunnel face. These interventions are easily performed in ground from the primary range of EPB shield application (Section 2.2.5) due to high capillary forces in this type of ground. The interventions become more complicated in the case of coarse ground from the extended application range. It is preferred to perform the interventions within jet grouting blocks. The jet grout block stabilizes the subsoil while excess air pressure prevents groundwater flow into the excavation chamber. Another available approach is to temporarily fill the excavation chamber of the EPB shield with a slurry to create a slurry filter cake, which seals the tunnel face for compressed-air application.

In general, ordinary compressed-air interventions are subjected to the health and safety regulations of most countries, which set safety limits on allowed air pressure values, allowable timespan for working in compressed air and required decompression time. If higher compressed-air pressure for tunnel face stabilization is required, the workers are required to enter the excavation chamber while breathing a special gas mixture, e.g. TRIMIX [Holzhäuser et al., 2006]. Additional option exists for slurry shields. The slurry in the excavation chamber is not lowered and saturation divers are deployed. This measure is extremely difficult and costly and therefore reserved solely for special cases.

## 2.4 Requirements for a particular support medium

### 2.4.1 Bentonite slurry

The bentonite slurry suspension has two fundamental functions to fulfil for slurry shield tunnelling. Firstly it is a hydraulic means of conveying the spoil with the use of a pipe system. For this function, it is beneficial to keep the yield point and thus the apparent viscosity of the slurry as low as possible to simplify slurry pumping [Longchamp, 2005].

The second function of the slurry is to stabilize the tunnel face. Two viewpoints are distinguished; the global pressure transfer and local pressure transfer (micro-stability). The slurry's yield point is the most important parameter of the slurry involved in the analysis for both cases. The standardised approaches for determination of slurry properties can be found for instance in DIN 4126 (2013), Longchamp (2005) or Triantafyllidis (2004).

The interaction with the ground can be globally described with the help of an existing pressure gradient  $f_{s0}$ , which represents the decrease of slurry excess pressure over a meter of the penetration distance into subsoil.  $f_{s0}$  is a theoretical variable, since the penetration depth is usually much smaller than 1 m. The existing pressure gradient can be calculated from the equation below (Eq. (1) – Müller-Kirchenbauer, 1977) or experimentally determined.

$$f_{so} = \frac{3.5 \cdot \tau_f}{d_{10}} \quad (1)$$

With

$f_{so}$  Pressure gradient [kN/m<sup>3</sup>]  
 $\tau_f$  Yield point of the slurry [kN/m<sup>2</sup>]  
 $d_{10}$  Characteristic grain size of the soil (to be obtained from grain distribution curve) [m]

If the existing pressure gradient is to be determined experimentally based on the maximal penetration depth, the following Eq. (2) should be used.

$$f_{so} = \frac{\Delta p}{e_{max}} \quad (2)$$

With

$\Delta p$  Slurry excess pressure [kN/m<sup>2</sup>]  
 $e_{max}$  Maximal penetration distance of the slurry [m]

The existing support pressure gradient can predict whether the type of slurry pressure transfer on the tunnel face will be a filter cake (Fig. 8 – Case 1) or penetration zone (chapter 2.3). According to DIN 4126, a penetration zone forms if the existing support pressure gradient is lower than 200 kN/m<sup>3</sup>. The slurry infiltrates deeper into the soil (Fig. 8 – Case 2), thus reducing the “Effectively Acting Support Force”, the force that helps maintain stability of the soil wedge (for further reference see DIN 4126, 2013 and Anagnostou & Kovari, 1994). It is recommended to design the slurry properties to achieve support pressure gradients higher than 200 kN/m<sup>3</sup> (Fig. 8 – Case 1).

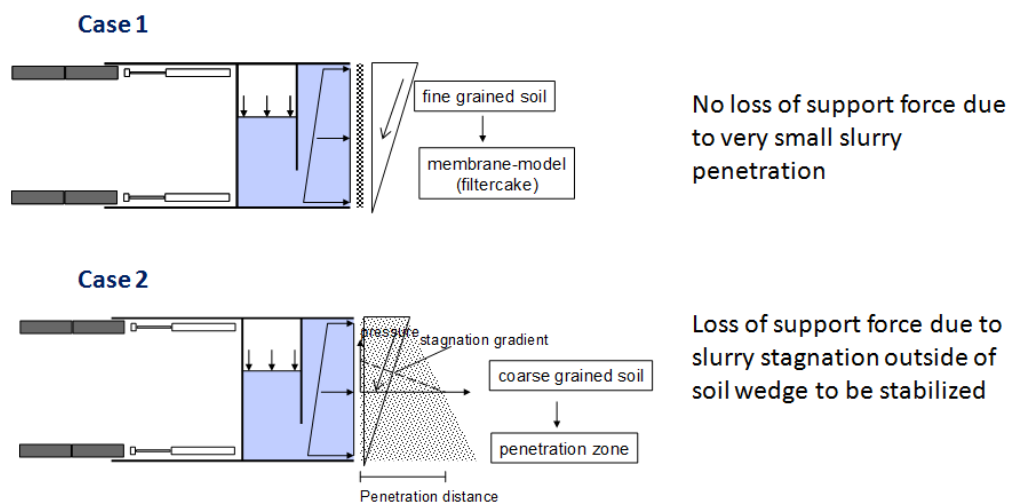


Fig. 8: Support force loss due to bentonite slurry infiltration: Case 1 – no loss, Case 2 –partial loss

From a local pressure transfer perspective, face stability is viewed at soil particle level. The required yield point of suspension assures the micro–stability (Broere, 2001). Micro-stability is the stability of a single or group of grains from falling out from the soil skeleton under gravity. The equation that defines the required yield point to satisfy the necessary criterion is found in DIN 4126 (Eq. (3)).

$$\frac{d_{10}}{2 \cdot \eta_F} \cdot \frac{\gamma_\varphi}{\tan(\varphi')} \cdot (1 - n) \cdot (\gamma_B - \gamma_F) \cdot \gamma_G \leq \tau_F \quad (3)$$

With

$d_{10}$	Characteristic grain size of the soil (to be obtained from grain distribution curve) [m]
$n$	Soil porosity [-]
$\gamma_B$	Unit weight of soil grains [kN/m <sup>3</sup> ]
$\gamma_G$	Partial safety factor for permanent load case in GZ1C acc. to DIN 1054 (= 1.00) [-]
$\gamma_F$	Unit weight of fresh slurry [kN/m <sup>3</sup> ]
$\gamma_\varphi$	Partial safety coefficient for drained soil within the status GZ1C in load case LF2 acc. to DIN 1054 (= 1.15) [-]
$\varphi'$	Characteristic drained friction angle of the soil [°]
$\eta_F$	Safety factor accounting for deviations in the yield point of suspension (= 0.6) [-]
$\tau_F$	Yield point of slurry [kN/m <sup>2</sup> ]

#### 2.4.2 Earth muck – EPB shield

The properties of earth muck in an EPB shield are more complex in comparison to a slurry suspension. The earth muck must contain defined properties that concern flow behaviour or consistency, internal friction or shear strength, stability, abrasiveness and tendency to clogging [Galli & Thewes, 2014]. Particular parameters of the earth muck are to be fulfilled in order to achieve its desired behaviour. Different parameters of the earth muck are required for the primary and extended application range of the EPB shields (Fig. 6).

The parameters for the primary application range (Fig. 6) of the EPB shields and their purposes are outlined in Tab. 1. The parameters were determined from laboratory investigations and are based on practical experience. In the primary application range, water may be used as a medium to adjust earth muck properties. In practice, foams are very often injected during excavation within this range to reduce stickiness of the earth muck and to improve compressibility of the muck.

Tab. 1: Required parameters of the earth muck to be used as the support medium within the primary application range,  $I_p$  denotes the plasticity limit and  $I_c$  the consistency index of soil [Thewes & Budach, 2010]

Parameter	Desired property of the support medium	Purpose	Reference
Permeability	$k < 10^{-5} \text{ m/s}$	To reduce groundwater inflow in the excavation chamber	Abe et al. (1978)
Good consistency for workability	$0.4 < I_c < 0.75$	To ensure flow behaviour	Maidl (1995)
Maintenance of the pressure gradient in the screw conveyer	$0.6 < I_c < 0.7$	To enable the pressure difference between excavation chamber and conveyor belt (shield interior)	Maidl (1995)
Good compressibility	dependant on the geological conditions of the ground and geometrical dimensions of the shield machine	To achieve homogeneous support	Maidl (1995)
Tendency to stick	$I_c < 0.5$ or $I_p < 20 \%$	To reduce stickiness	Maidl (1995), Hollmann (2012)
Wear effect	$I_c < 0.8$	To reduce wear	Maidl (1995)

Within the extended application range, the desired properties must be achieved by mixing the soil with additives, i.e. by soil conditioning. The additives used for soil conditioning are mostly foams, polymers or slurries of fines. They are injected through nozzles in front of the cutting wheel, in the excavation chamber and into the screw conveyer during excavation and stoppages.

The optimal amount of additives to be added to soils in extended application range can be determined by laboratory testing or based on practical experience [Vinai, 2006]. For testing of additives and mixtures consisting of ground and additives (i.e. conditioned soils) several methods have been developed. These methods are outlined in Tab. 2. The recommended values for the workability are investigated by a slump test aiming at a 10 – 20 cm slump [Galli & Thewes, 2014] and for the hydraulic conductivity of the earth muck with  $k < 10^{-5}$ -  $10^{-4} \text{ m/s}$ . For the other testing procedures and parameters from Tab. 2, no guide values are available. These results must be evaluated based on experience. For the further details about the outlined testing procedures, see the provided references in Tables 1 and 2.

Tab. 2: Tests performed on additives or conditioned soils from the extended application range of the EPB shields

Type of test	Tested material	Purpose of the test	Reference
Drainage test	Foam	To check the stability of the foam	Vinai (2006), Budach (2012)
Density	Foam	Foam density and actual foam expansion ratio	Budach (2012)
Mixing test	Conditioned soil	Reduction in friction, torque measurement	Quebaud et al. (1998)
Slump test	Conditioned soil	Good workability	Thewes et al. (2010), Vinai (2006)
Permeability test	Conditioned soil	To control the water ingress into the excavation chamber	Bezuijen et al (1999), Maidl (1995)
Screw conveyor test	Conditioned soil	To determine the achievable pressure drop along the screw conveyor	Bezuijen & Schaminée (2001), Merritt & Mair (2006), Peila et al. (2007)
Stability	Conditioned soil	Development of workability over time	Vinai (2006)

### 3 German safety concept for tunnel face stability

Two operational limits for the support pressure are defined in the German regulation ZTV-ING (2012): the lower and the upper limit (RiL 853 references ZTV-ING regarding support pressure calculations).

The lower support pressure limit has to ensure a minimal support force ( $S_{ci}$ ), which consists of two components and their respective safety coefficients (Eq. (4)). The first component of the support force ( $E_{max,ci}$ ) has to balance the earth pressure, and is calculated here based on active kinematical failure mechanism of the tunnel face (section 4.1). The second component of the support force ( $W_{ci}$ ) has to balance the groundwater pressure and is determined based on the elevation of groundwater level above the tunnel crown.

$$S_{ci} = \eta_E \cdot E_{max,ci} + \eta_W \cdot W_{ci} \quad (4)$$

With

$\eta_E$	Safety factor for earth pressure force (= 1.5) [-]
$\eta_W$	Safety factor for water pressure force (= 1.05) [-]
$S_{ci}$	Required support force (circular tunnel face) [kN]
$E_{max,ci}$	Support force due to earth pressure (circular tunnel face) [kN]
$W_{ci}$	Support force due to groundwater pressure (circular tunnel face) [kN]

The upper support pressure limit is defined as a limiting pressure to avoid a break-up of the overburden or blow-out of the support medium. Therefore, the maximal support pressure has to be smaller than 90 % of the total vertical stress at the tunnel crown.

Break-up/ blow out safety:

$$1 \leq \frac{0.9 \cdot \sigma_{v,crown,min}}{S_{crown,max}} \quad (5)$$

With

$\sigma_{v,crown,min}$	Total vertical stress in the tunnel crown considering minimal unit weight of soil [kN/m <sup>2</sup> ]
$S_{crown,max}$	Maximal allowable pressure in the tunnel crown due to break up safety / blow-out safety [kN/m <sup>2</sup> ]

The operation range of support pressure defined by the two limits is visualized in Fig. 9. The two limits are generally valid for all types of shield machines and tunnel advance phases, i.e. excavation, stoppage, standstill. There are distinctions between machine types regarding the support pressure deviations that should be considered, i.e. +/- 10 kPa for the slurry shield (including compressed air support) and +/- 30 kPa for the EPB shield.

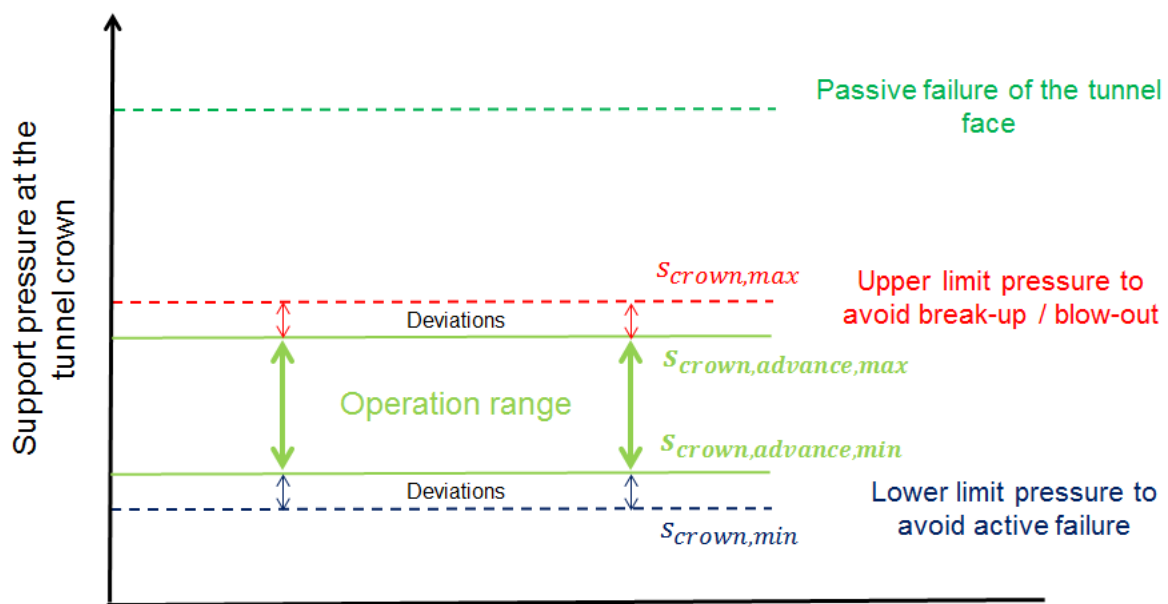


Fig. 9: Allowable operational pressures at the tunnel crown of a shield machine

Furthermore, it is recommended in ZTV-ING (2012) to consider different unit weight of soil for the calculation of minimal support pressure (lower limit) and of the blow-out (upper limit). The average unit weight, as defined by the geotechnical consultant, should be used for the lower limit and the minimal unit weight for the upper limit. ZTV-ING (2012) additionally prescribes in case of compressed-air support that the support pressure at the lowest point of air contact with the tunnel face must have a minimal safety factor of  $\eta = 1.05$  compared to the local groundwater pressure.

ZTV-ING (2012) further defines for slurry face support that the effectiveness of the slurry support mechanism and the local stability have to be investigated according to DIN 4126 (Section 2.4.1).

## 4 Calculation methods for determination of the required support pressure due to the acting earth pressure

Various methods to determine the required support pressure due to the acting earth pressure can be found in literature. All available approaches can be divided into four fundamental groups:

- Analytical methods
- Empirical methods
- Experimental methods
- Numerical methods

The outlined calculation methods concerning the ultimate limit state approach are presented in the following sections. The aim of this chapter is to present the state of the art of the calculation methods.

### 4.1 Analytical

The group of analytical methods includes limit equilibrium and limit state methods. These methods assume a possible failure mechanism of the tunnel face or a stress distribution in the ground respectively and from that determine a support pressure at collapse. Common features of most of the analytical methods are based on the adoption of two widely used laws of failure in soil mechanics. On one hand, the Mohr-Coulomb law of failure is broadly adopted for frictional or frictional-cohesive materials where the associated flow rule is dominating among the formulations. On the other hand, Tresca law of failure (associated) is mostly applied for purely cohesive materials.

The limit equilibrium methods can be characterised by the required assumption of a kinematical failure mechanism of the tunnel face. The first limit equilibrium failure mechanism was suggested by Horn (1961) and assumes a sliding wedge in front of the tunnel face that is loaded by a rectangular prism stretching up to the terrain surface level (Fig. 10). This sliding wedge mechanism for investigation of tunnel face stability was introduced to mechanised tunnelling by Anagnostou & Kovari (1994) and Jancsecz & Steiner (1994). The equilibrium condition of the stabilizing and destabilizing forces is formulated on the sliding wedge. The wedge's weight and the load from the overlying prism are listed as destabilizing forces. Stabilizing forces retain movements of the wedge and thus the tunnel face collapse. The stabilizing forces are composed of the tunnel face support force and shear resistance forces at boundary planes of the failure mechanism. Moreover, an assumption of the horizontal earth pressure acting on the vertical triangular planes of the wedge is needed to determine the shear resistance on them. Recently, Anagnostou (2012) suggested a method that eliminates the required assumption of horizontal stresses on the triangular planes. The method originates from the method of slices [Walz, 1983] and formulates the equilibrium condition on an infinitively slim horizontal slice of the wedge. The equilibrium condition is subsequently integrated over the whole wedge. Hu et al. (2012) generalized the shape of the sliding wedge and of the overlying prism to allow for a variable width along their vertical axis. Furthermore, the boundaries of the failure mechanism do not necessarily have to have a planar shape as Mohkam (1989) suggested a failure wedge with inclined slide surface consisting of a logarithmic spiral. The commonly in practice used limit equilibrium formulations will be presented in detail in the section 6.1.

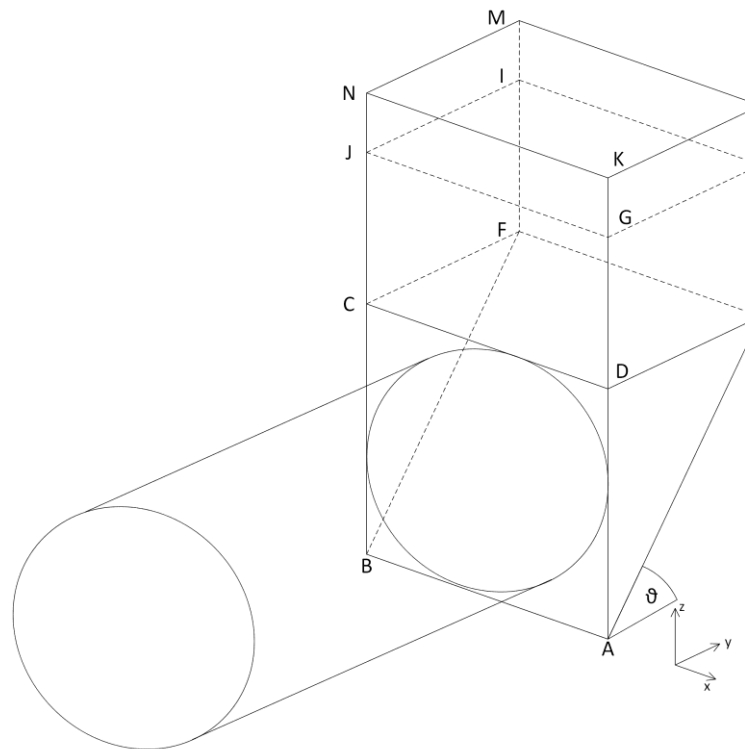


Fig. 10: Horn's failure mechanism with the wedge (ABCDEF) and prism (CDEFKLMN) considering groundwater level (GHIJ)

Various solutions for the tunnel face stability have been formulated based on bound theorems within the plasticity theory. This group of approaches is often known as "limit state methods". The solution for the tunnel face stability can be obtained by adopting the upper or the lower bound of the plasticity theory.

The upper bound theorem is also known as the kinematical solution [Kolymbas, 2005] based on plasticity theory, as it assumes a kinematically possible failure mechanism. Adopting the upper bound solution, the tunnel face will collapse as if the work done by the failure mechanism and by external forces acting on it is higher than the work done by internal stresses [Kirsch, 2009]. Unfortunately, this approach will give a lower value of support pressure at collapse than what is actually needed in reality. Therefore the upper bound solution is always taken to be on the unsafe side compared to reality.

The lower bound solution signifies a static approach based on plasticity theory. The lower bound solution of the tunnel face stability is found by determining a statically admissible stress distribution within a soil body that balances the external forces at the boundaries of the body without the yield being exceeded in any point of the soil body [Yu, Sloan et al., 1998]. The lower bound solution always delivers a higher support pressure than at actual tunnel face failure.

In summary, it can be expressed, that if the applied support pressure is higher than the pressure obtained by the lower bound theorem, the tunnel face will not collapse. The tunnel face will collapse if a lower pressure is applied than what is calculated by the upper bound theorem. The tunnel face may be stable if a tunnel face pressure between upper and lower bound is applied.

Davis et al (1980) developed both upper and lower bound stability solutions for a tunnel heading through purely cohesive soil assuming undrained conditions. In order to describe the real behavior of the tunnel, they investigated three different cases that included two simplified cases and one with real three dimensional tunnel geometry (Fig. 11 to Fig. 13):

- 1) Plane strain unlined tunnel – approximates infinitely long tunnel (Fig. 11)
- 2) The plane strain heading – approximates infinitely wide tunnel (Fig. 12)
- 3) Cylindrical tunnel heading – only lower bound solution derived – attempt to describe real conditions (Fig. 13)

Next to global failures, Davis et al (1980) also assessed the possibility of a “local failure mode” of a tunnel face, which denotes a rotation of a hemisphere on the tunnel face without any dependence on actual support pressure but only on the support pressure gradient in vertical direction.

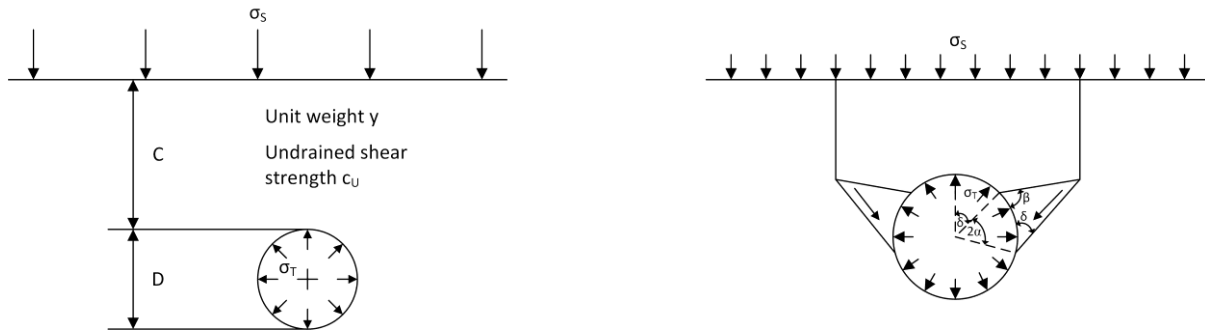


Fig. 11: Plane strain unlined tunnel [Davis et al., 1980]

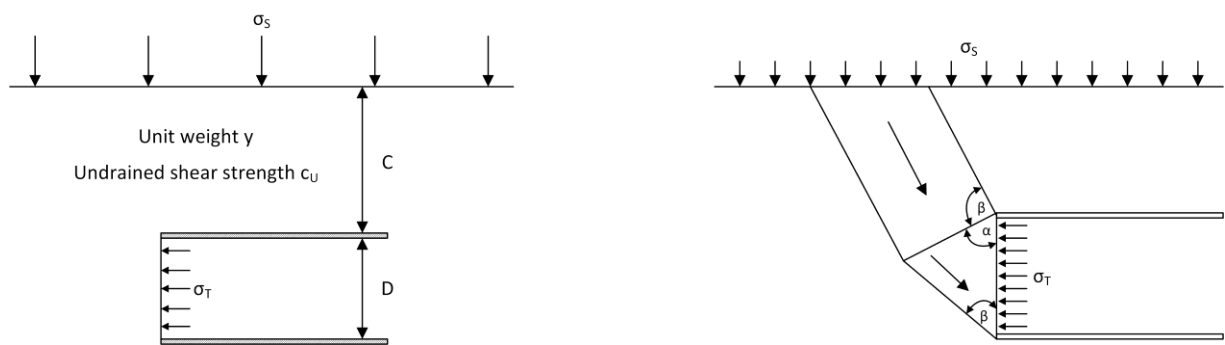


Fig. 12: The plane strain heading [Davis et al., 1980]

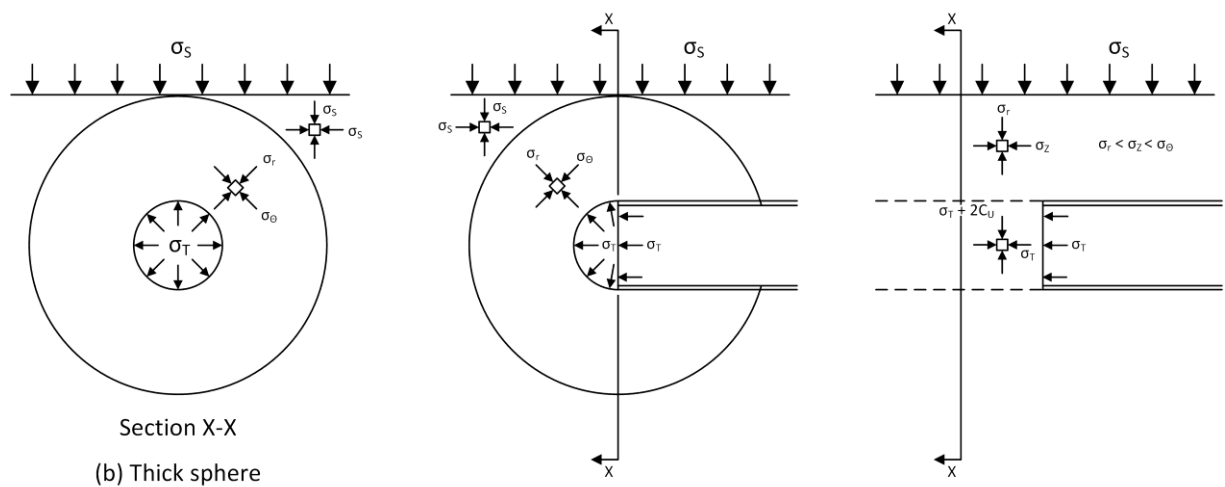


Fig. 13: Cylindrical tunnel heading [Davis et al., 1980]

The authors determined for each case the critical stability ratio (for the origin of the critical stability ratio approach see section 4.2) while adopting one of the bound theorems. The stability ratio is generally calculated as a subtraction of vertical stress at the tunnel axis and the support pressure divided by the undrained shear resistance of soil. When the stability ratio achieves the critical ratio, the tunnel collapses. Davis et al (1980) found that the critical stability ratio is variable, contrary to Broms & Bennemark (1967), since it depends on the ratio between overburden and tunnel diameter (Fig. 14).

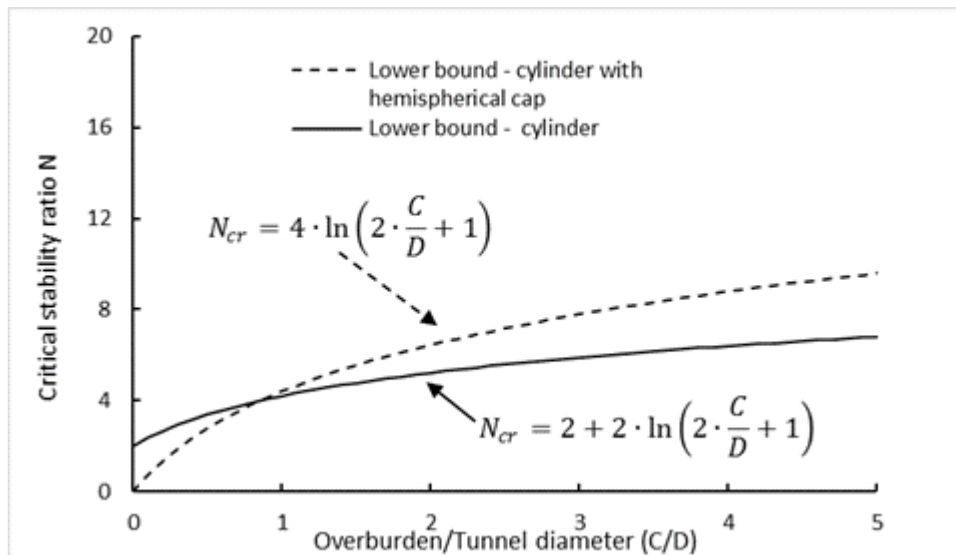


Fig. 14: Critical stability ratios based on lower bound solution of 3D cylindrical tunnel heading [Davis et al., (1980)]

Davis et al (1980) concluded with the consideration of experimental centrifuge test results (Mair, 1979) that actual collapse pressures can be found “fairly exactly” by adopting the lower bound solution for case 3 – cylindrical tunnel heading (Fig. 13 and Fig. 14). However, these results cannot be completely generalized as the authors recommended to use the suggested approach for tunnels with an overburden/tunnel diameter ( $C/D$ ) ratio lower than 3. The critical stability ratio for local failure mode for cylindrical tunnel heading adopting the upper bound amounts to 10.96.

Leca & Dormieux (1990) formulated the upper and lower bound solutions of the face stability for excavation through frictional soils and frictional - cohesive soils by adopting the Mohr-Coulomb law failure and the assumption of drained conditions. They investigated three possible failure modes of the tunnel face by assuming multiple conical rigid blocks (Fig. 15) as the failure mechanism. These blocks had an elliptical cross-section at the intersection of the tunnel face. The collapse support pressures were calculated for the active failure and blow-out. It should be noted that Leca & Dormieux (1990) were actually investigating the pressure at passive failure of the tunnel face instead of the blow-out pressure of the support medium. Subsequently, the authors compared the theoretically calculated face pressures at collapse with experimentally obtained values by Chambon & Corte (1989). Leca & Dormieux (1990) concluded that there was a close agreement between upper bound solutions and experimental results. The calculated results also showed that the surcharge on the terrain surface had a minor influence on the tunnel face stability in frictional or frictional-cohesive soils.

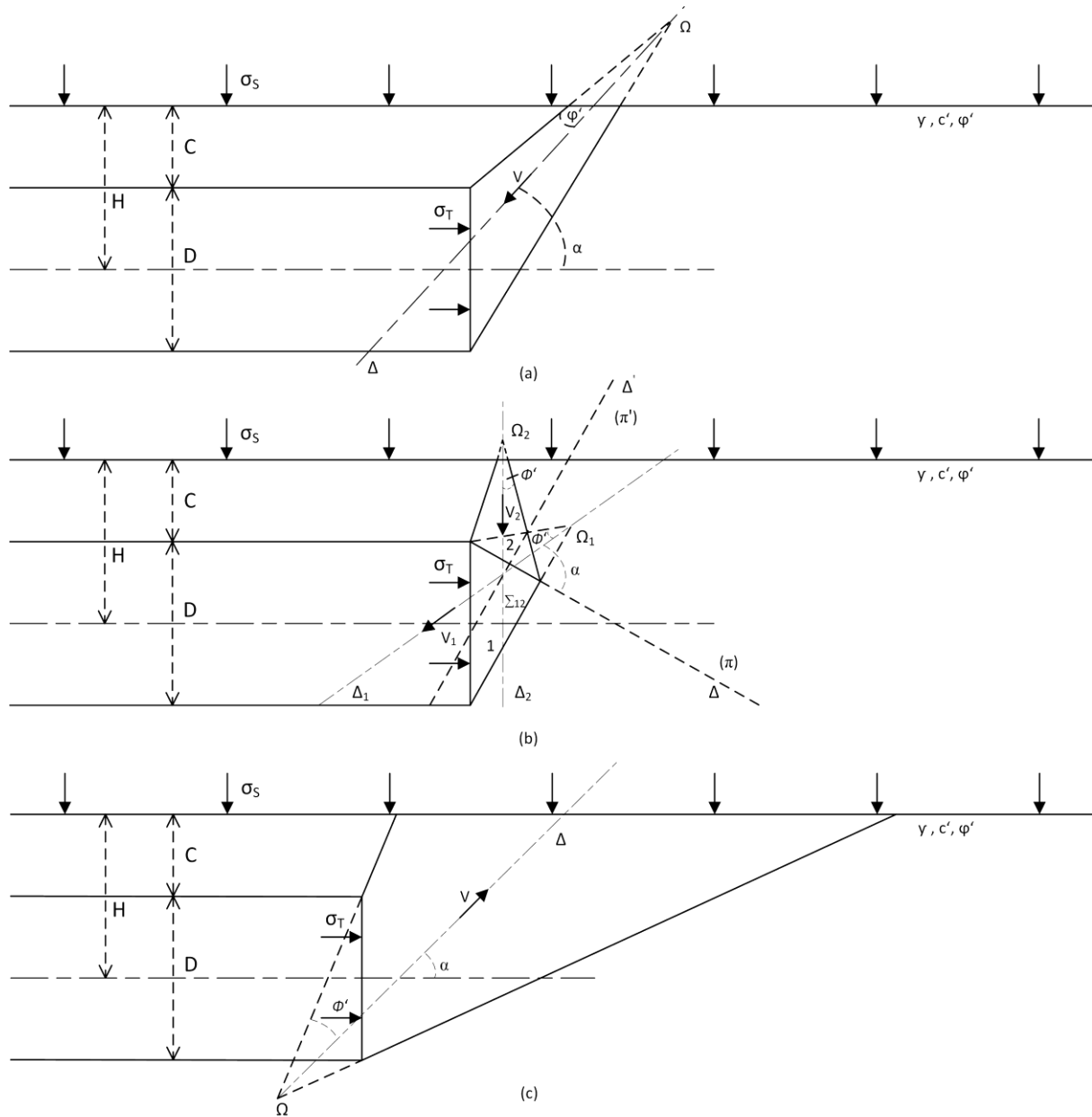


Fig. 15: Upper bound failure mechanisms [Leca & Dormieux, 1990]

Mollon et al. (2010) recently suggested a further upper bound solution (Fig. 16). The authors developed a failure mechanism that is similar to Leca & Dormieux (1990) but takes the collapse of the whole tunnel face into account (Fig. 16). This calculation approach allows for the adaptation of a tension cut-off for the soil parameters. In most recent development, Senent et al. (2013) implemented a possible method to consider the Hoek-Brown failure condition (for rock) within the failure mechanism suggested by Mollon et al. (2010).

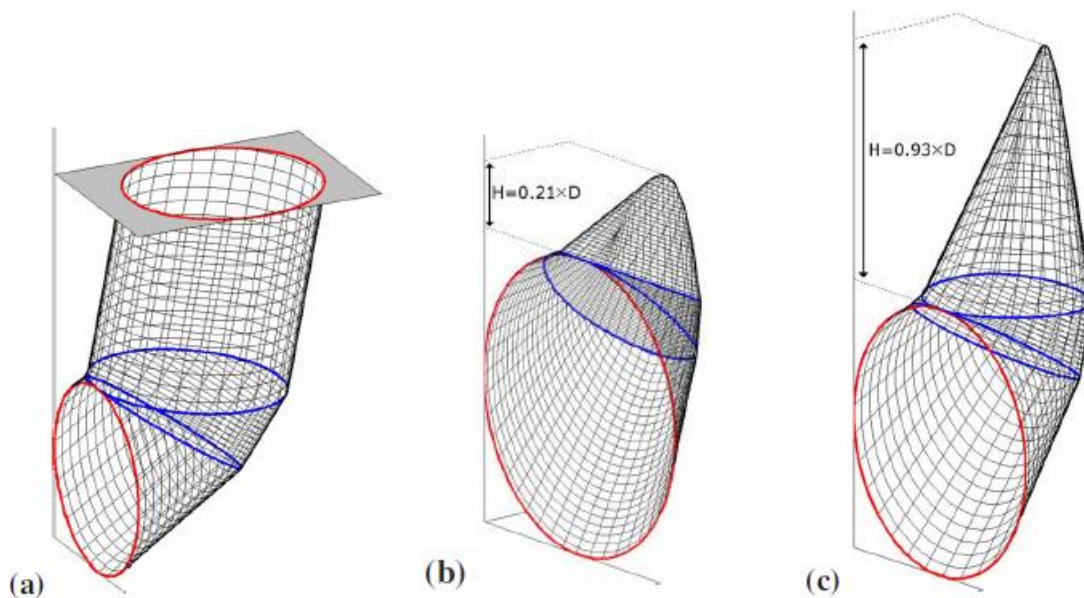


Fig. 16: Variability of the failure mechanism suggested by Mollon et al.: a)  $\varphi = 0^\circ$  and  $c = 20 \text{ kN/m}^2$ ,  $C/D = 1$ ; b)  $\varphi = 30^\circ$  and  $c = 0 \text{ kN/m}^2$ ;  $C/D \geq 0.5$ ; c)  $\varphi = 17^\circ$  and  $c = 7 \text{ kN/m}^2$ ;  $C/D \geq 1$  [Mollon et al., 2010]

## 4.2 Empirical and experimental methods

The second methodological group is represented by empirical approaches to determine the tunnel face pressure. Empirical solutions for the tunnel face stability are usually derived based on experiments [Broms & Bennermark, 1967] or numerical calculations [Vermeer, 2002]. The stability ratio method by Broms & Bennermark (1967) represents the most important calculation approach from empirical methods.

Broms & Bennermark (1967) conducted laboratory experiments that investigated the extrusion stability of a clayey soil to understand why a serious accident happened when a clayey soil mass slid through a vertical circular opening in a sheet pile wall (Fig. 17).

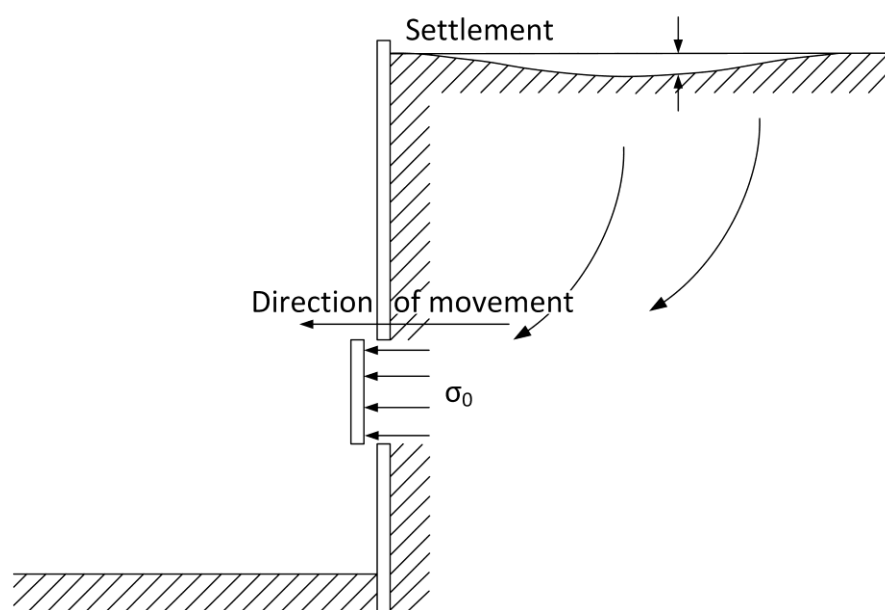


Fig. 17: Layout of a circular opening in the vertical sheet pile wall [Broms & Bennermark, 1967]

Broms & Bennermark (1967) developed an equation describing the soil stability behind similar vertical openings based on a stability ratio ( $N$ ) (Eq. (6)). The stability ratio depends on the subtraction of the pressure supporting the opening ( $s_{axis}$ ) from the vertical stress ( $\sigma_{v,axis}$ ) at the opening axis then divided by the undrained shear strength ( $c_u$ ) of the soil. As expected, the approach assumes undrained conditions and purely cohesive soil behavior (Tresca material). The direct subtraction of the vertical stress and horizontal support pressure can be carried out since the coefficient of lateral pressure is here equal to 1.

$$N = \frac{\sigma_{v,axis} - s_{axis}}{c_u} \quad (6)$$

Subsequently, Broms & Bennermark (1967) performed multiple laboratory experiments and concluded that the soil within a vertical opening is stable if the stability ratio is lower than 6. They suggested to apply the developed method for investigation of tunnel heading stability.

Other theoretical works dealing with tunnel face stability were validated by experimental results. The theoretical model developed by Davis et al (1980) was supported with centrifuge experiments conducted by Mair (1979) for undrained conditions of purely cohesive soil. Furthermore, Leca & Dormieux (1990) derived a theoretical model for frictional-cohesive materials that referred to the experimental simulations of tunnels driven in dry sand by Chambon & Corte (1989 & 1994). Among limit equilibrium methods, the formulation by Anagnostou & Kovari (1994) achieved the best correlation with experimental investigation as referred to by Messerli & Anagnostou (2010) and Bezuijen & Messemackers-van de Graaf (1997) (cited by Broere, 2001) or the formulation of Jancsecz & Steiner (1994) examined by Plekkenpol et al (2005) on saturated sand.

Generally, two main groups of experimental devices for investigation of the face stability are described in literature. These groups are different by the amount of gravity load applied. Therefore, they are called 1-g experiments and n-g experiments. The advantages and disadvantages of both groups were summarized e.g. by Kirsch (2009):

- 1-g experiments – Experimental devices can be larger, therefore less problems will occur due to the grain size effect. Low stress levels are present which make it complicated to determine actual material properties of the investigated frictional material. Therefore, the numerical model calibration based on 1-g experiments is problematic. The 1-g devices may be more sophisticated, e.g. by Berthoz et al. (2012) simulating an EPB shield including screw conveyor and cutting wheel (Fig. 18). Furthermore, a sophisticated measuring devices can be implemented, e.g. for the investigation of soil arching and stress release during tunnel face collapse [Chen et al., 2013].

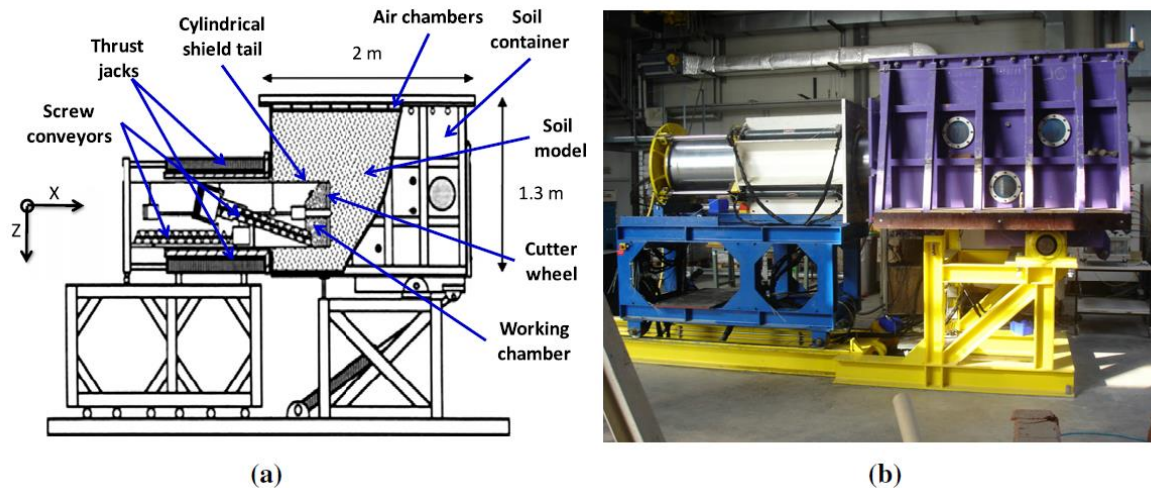


Fig. 18: Sectional diagram (a) and photograph (b) of the EPB shield model [Berthoz et al., 2012]

- n-g experiments (centrifuges, Fig. 19) – the experimental devices are much smaller than real tunnels; therefore an influence of the grain size effect should be considered in the evaluations of frictional materials. Centrifuge tests are useful to investigate purely cohesive materials under undrained conditions such as clays. In the case of clays, the size factor of the grains is not an important factor. Generally the grain size influence can be neglected for a tunnel diameter larger than 0.1m with sand grains smaller than 0.2 mm. The advantage of n-g experiments is that real stress conditions can be created, so that soil consolidation phenomena can be considered.



Fig. 19: Model assembly of a centrifuge experiment [Idinger et al., 2011]

#### 4.3 Numerical

The aim of numerical face stability analysis is to find the highest support pressure at which the active failure of the tunnel face occurs (collapse). The four following methods are available to achieve this failure (Kirsch, 2009; Vermeer et. al, 2002, Zhang et al., 2011):

- 1) Load reduction method – face support pressure is reduced until the failure occurs.
- 2) Strength reduction method – shear properties of the soil are reduced until the failure occurs.

- 3) Displacement control method – displacement of the tunnel face towards the cavity is increased until the failure occurs.
- 4) Centrifuge model testing-based method – gravitational acceleration is increased until the failure occurs.

The displacement control method is usually used for laboratory experiments verification. The load reduction method is generally more advantageous compared to strength reduction method. In the load reduction method, the material parameters of soils are not changed during the calculations, so the obtained failure shape is closer to reality.

For numerical modelling, a suitable constitutive law for soil must be chosen. The linear elastic – perfectly plastic model with Mohr-Coulomb yield condition is usually evaluated as being sufficiently accurate to determine the support pressure during failure (Kirsch, 2010). The non-associated flow rule may be assumed in calculations.

CAUTION: Large terrain surface deformations will happen if the tunnel progress takes place with a face pressure determined by these numerical methods. The methods mentioned here are only employed for the investigation of the face stability. They are not to be confused with methods used in practice for investigation of machine–ground interaction presented in section 6.3.

#### 4.4 Summary

Various methods used to investigate the face stability and determine the face support pressure at collapse were developed in the last decades. Based on these methods, the support pressures were calculated and the obtained values were successfully applied with consideration of safety coefficients during tunnel excavations. The theoretically calculated pressures at tunnel face collapse were not validated in practice with real scale experiments. Only laboratory experiments were used to validate the particular calculation methods. This section aims to summarize the developed methods with regard to their correlations with experimental results. Moreover, the information about their use in practice is provided based on authors' experience.

Depending on the soil type, the soil can show drained or undrained behaviour during excavation. Therefore, particular calculation methods are fitted to certain ground conditions. For drained conditions, the best fit between theoretical calculations and experiments is found for limit equilibrium methods formulated by Anagnostou & Kovari (1994) or Jancsecz & Steiner (1994) and the limit state upper bound solution by Leca & Dormieux (1990). However, the upper bound calculations become complicated when the failure mechanism is close to the reality. Thus, various formulations of limit equilibrium on the sliding wedge are commonly used in practice. For undrained soils, the lower bound limit state method assuming a cylindrical tunnel model was the best predictor of the support pressures at collapse [Davis et al., 1980]. The authors determined required support pressures by using the stability ratio approach [Broms & Bennermark, 1967]. This calculation method is very straightforward, and its concepts have become a standard for excavations in purely cohesive soils.

In accordance with this summary, the limit equilibrium methods and stability ratio methods will be presented in chapter 6. In chapter 8 additional background for in practice relevant support pressure calculations is presented with calculation examples.

## 5 Calculation methods for determination of required support pressure due to the acting water pressure

Generally, it is required in closed face shield tunnelling that the support pressure has to balance or be higher than the groundwater pressure. This requirement is reasonable since it avoids unwanted flow towards the tunnel face which can cause surface settlements. The support force due to groundwater pressure is easy to calculate (Eq. 7). Care must be taken, that the support pressure exceeds the water pressure at all locations of the tunnel face.

$$W_{ci} = \gamma_w \cdot h_{w,axis} \cdot \frac{\pi D^2}{4} \quad (7)$$

With

$h_{w,axis}$  Groundwater level above the tunnel axis [m]

$\gamma_w$  Unit weight of water [kN/m<sup>3</sup>]

D Tunnel diameter [m]

$W_{ci}$  Groundwater-pressure force (circular tunnel face) [kN]

In some cases of EPB excavations (in open or transition mode), there is an attempt to decrease the support pressure below the groundwater pressure to reduce wear of the machine. Hence, groundwater flows towards the tunnel face. Consequently, the groundwater flow effects must be considered as additional forces destabilizing the tunnel face [Anagnostou & Kovari, 1996] in the matter of effective stresses (Fig. 20). The amount of the destabilizing force due to groundwater flow is primarily defined by the difference in piezometric heads between excavation chamber and subsoil. Furthermore, the difference in ground permeability and of conditioned soil within the excavation chamber also plays a role [Budach, 2011].

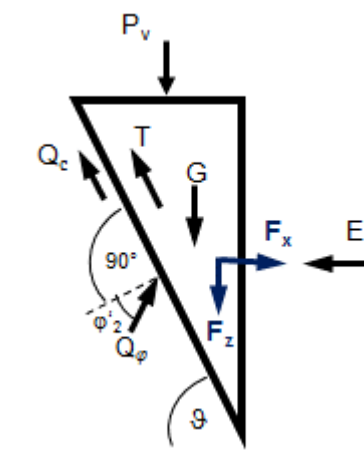


Fig. 20: Sliding wedge acc. to Horn with additional forces due to the groundwater flow ( $F_x$  and  $F_z$ ) according to [Anagnostou & Kovari, 1996], for explanation of other forces see Fig. 21

## 6 Face support pressure calculation in practice

Excavation generally creates a change from the primary stress state in the ground to a secondary stress state. The stress change is influenced by the ratio of applied support pressure and the original stress state in the ground. The change in stress state determines the ground deformations that occur due to the shield drive. Furthermore, the stress change on the tunnel face has a primary influence on further interactions of the shield and ground during excavation and between the lining and ground at the final stage.

Two representatives of the most commonly used “Ultimate Limit State Approaches” in tunnelling practice will be presented in detail in this chapter. First, the possible formulations of limit equilibrium on the sliding wedge will be outlined. Second, the calculation approach adopting stability ratio method will be presented in this chapter. Moreover, numerical methods as a representative of practice relevant “Serviceability Limit State Approaches” will be discussed.

The “Ultimate Limit State Approaches” introduced in sections 6.1 and 6.2 may be generally used for support pressure calculations during shield passages under “green fields” for all excavation stages (excavation, stoppage, intervention). Additional examination of deformations by numerical analysis (section 6.3) is highly recommended for tunnels under sensitive surface constructions.

### 6.1 Limit equilibrium method

Face stability calculations in practice are typically performed using the limit equilibrium method when the soil on the face is either non-cohesive or with alternating cohesive and non-cohesive layers. The effective (drained) shear parameters of a soil are assumed in this case. It is generally not recommended to use the limit equilibrium approach for calculations with undrained shear soil parameters.

The first step of the calculation is represented by the definition of the failure mechanism (Fig. 21). The circular tunnel face can be approximated with a square whose edge length is equal to the shield diameter [Jancsecz & Steiner, 1994], as a first option. The second option is to approximate the circular tunnel face with a square of the same cross sectional area as the circular tunnel face [Anagnostou & Kovári, 1994]. Thereby, the front plane of the sliding wedge is defined (Fig.21). For simplicity, the formula adopting the edge length equal to the diameter will be followed in the upcoming examples.

Once the sliding wedge is assumed, the forces acting on it can be determined (including the support force). The forces must be in a limit equilibrium, meaning that the bearing capacity of the wedge is just fully mobilized. The support force and the mobilized soil shear resistance act as stabilizing forces, while the wedge’s own weight and weight of the overlaying prism cause destabilizing forces. The equilibrium conditions are formulated on the inclined sliding surface (Fig. 21) in perpendicular and in parallel direction.

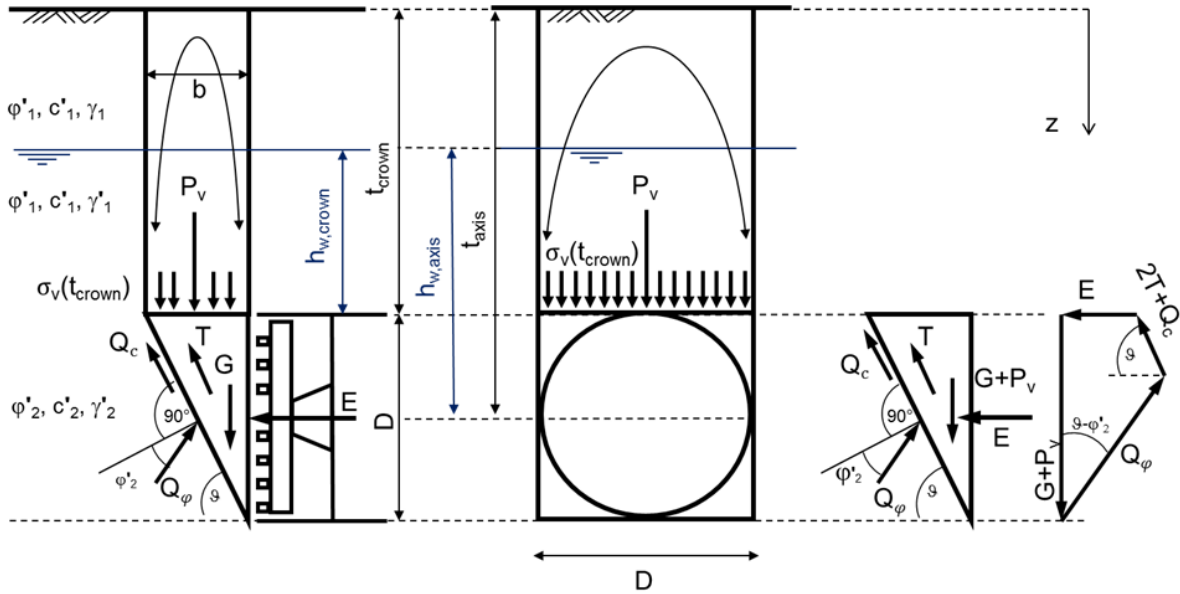


Fig. 21: Forces acting on the wedge with  $E_{re}$  = support force due to the earth pressure,  $G$  = own weight of wedge,  $P_v$  = vertical load from the soil prism,  $T$  = Shear force on the vertical slip surface,  $\vartheta$  = Sliding angle,  $\varphi'$  = Friction angle of soil,  $c$  = cohesion of the soil,  $D$  = shield diameter and  $Q$  = shear force on inclined surface,  $\gamma$  = unit weight of soil.

By summing two equilibrium conditions, the required support force can be calculated by equation (8). The summarized equilibrium condition is expressed dependant on the sliding angle of the wedge ( $\vartheta$ ) as its critical value is not yet known.

$$E_{re}(\vartheta) = \frac{(G + P_v) \cdot (\sin(\vartheta) - \cos(\vartheta) \cdot \tan(\varphi'_2)) - 2 \cdot T - c'_2 \cdot \frac{D^2}{\sin(\vartheta)}}{\sin(\vartheta) \cdot \tan(\varphi'_2) + \cos(\vartheta)} \quad (8)$$

Subsequently, the critical sliding angle ( $\vartheta_{crit}$ ) of the wedge has to be found for which the highest support force ( $E_{max,re}$ ) is required. Thus the maximization of the support force is performed by a variation of the sliding angle (Fig. 22).

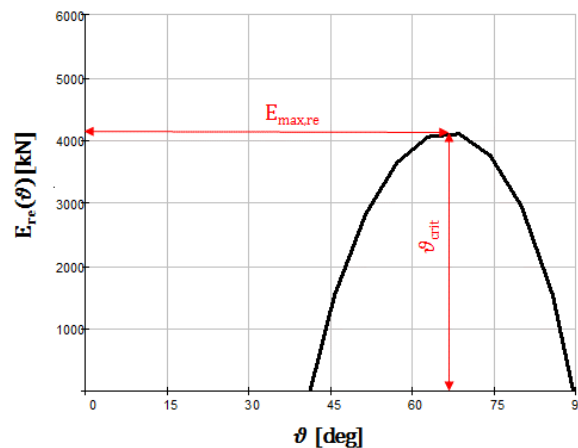


Fig. 22: Example of the determination of the highest required support force ( $E_{max,re}$ ) by variation of the sliding angle ( $\vartheta$ ).

The critical sliding angle can also be found when the first derivative of the support force function equals zero (Eq. (9)).

$$\frac{dE_{re}(\vartheta_{crit})}{d\vartheta} = 0 \quad (9)$$

From this point onward, determination of variables for equation (8) is shown. Assumptions used to determine particular forces vary among authors. The following pages explain a variety of available options for those calculations.

Two options are available to determine the force  $P_v$  acting on the wedge by the prism's weight.  $P_v$  can be calculated by multiplying the area on top of the wedge with the vertical effective stress acting on the wedge (Eq. (10)).

$$P_v = A \cdot \sigma_v(t_{crown}) = D \cdot \frac{D}{\tan \vartheta_{crit}} \cdot \sigma_v(t_{crown}) \quad (10)$$

$P_v$	Vertical load force from the soil prism on the wedge
$\sigma_v(t_{crown})$	Vertical surcharge from the prism on the wedge
A	Cross-sectional area of the silo / of the top of the wedge [m <sup>2</sup> ]

The stress is found considering the full weight of the overburden (Eq. (11)) or accounting for a soil arch above the wedge according to Janssen's silo theory (1895) that leads to a decrease in vertical stress (Eq. (12)). The criterion used to select between the two approaches is defined by the overburden height. If the overburden height is lower than twice the tunnel diameter, the full weight of the overburden is applied. Janssen's silo theory may be adopted if the overburden is higher. However, Anagnostou & Kovári (1994) suggest always using the Janssen's equation. The coefficients of the lateral earth pressure at the lateral planes of the silo vary significantly among different authors (Tab. 3). The authors of this recommendation suggest to use the coefficient according to Melix (1987) based on extensive practical experience.

$$\sigma_v(z) = \gamma_{1,av} \cdot z + \sigma_s \text{ for } t_{crown} \leq 2 \cdot D \quad (11)$$

With

$\sigma_v(z)$	Vertical stress at the elevation z [kN/m <sup>2</sup> ]
$\gamma_{1,av}$	Average soil unit weight in the overburden area [kN/m <sup>3</sup> ]
z	Vertical coordinate starting from the terrain surface [m]
$t_{crown}$	Overburden height [m]
$\sigma_s$	Surcharge on the surface (traffic load) [kN/m <sup>2</sup> ]

$$\sigma_v(z) = \frac{A}{K_1 \cdot \tan(\varphi'_1)} \cdot \gamma_{1,av} - c'_1 \cdot \left(1 - e^{-\frac{U}{A} \cdot K_1 \cdot z \cdot \tan(\varphi_1)}\right) + \sigma_s \cdot e^{-\frac{U}{A} \cdot K_1 \cdot z \cdot \tan(\varphi'_1)} \quad (12)$$

for  $t_{crown} > 2 \cdot D$

With

A	Cross-sectional area of the silo / of the top of the wedge [m <sup>2</sup> ]
U	Circumference length of the silo [m]
K <sub>1</sub>	Coefficient of lateral earth pressure within the silo (see Tab. 3) [-]

Tab. 3: Suggested coefficients for the lateral earth pressure within the silo K<sub>1</sub> ; where denotes: k<sub>a</sub> the coefficient of active lateral earth pressure, k<sub>p</sub> the coefficient of passive lateral earth pressure and k<sub>0</sub> the coefficient of earth pressure at rest

Author	Assumed coefficient of the lateral earth pressure
Terzaghi & Jelinek (1954)	$K_1 = 1.0$
Melix (1987)	$K_1 = 0.8$
Anagnostou & Kovári (1994)	$K_1 = 0.8$
Jancsecz & Steiner (1994)	$K_1 = k_a = \left(\tan\left(45 - \frac{\varphi'_1}{2}\right)\right)^2$
Mayer, Hartwig, Schwab (2003)	$K_1 = 1.0$ if $t_{crown} \leq 5 \cdot d$
Kirsch & Kolymbas (2005)	$K_1 = k_0 = 1 - \sin(\varphi'_1)$
Girmscheid (2008)	$k_a < K_1 < k_p$ , $K = 1$ recommended

The force G, which describes the wedge's own weight, is defined by Eq. (13).

$$G = \frac{1}{2} \cdot \frac{D^3}{\tan(\vartheta_{crit})} \cdot \gamma_{2,av} \quad (13)$$

With

G	Own weight of the wedge [kN]
D	Tunnel diameter [m]
$\gamma_{2,av}$	Average soil unit weight in the tunnel face area [kN/m <sup>3</sup> ]

The most contentious point in the limit equilibrium calculation approach is the determination of the shear resistance force on the vertical triangular planes of the wedge. The shear resistance force consists of two components, the friction force and cohesion force (Eq. (14)).

$$T = T_R + T_c \quad (14)$$

With

$T$	Shear resistance force on the vertical triangular plane of the wedge [kN]
$T_R$	Shear resistance force due to friction [kN], alternatively $T_{R,1}$ or $T_{R,2}$ see Eq. (16) and (17)
$T_c$	Shear resistance force due to cohesion [kN]

On a one hand, the relative agreement exists about the formulation of the cohesion component since it is independent of the lateral earth pressure acting on the wedge (Eq. 15).

$$T_c = \frac{c_2 \cdot D^2}{2 \cdot \tan(\vartheta_{crit})} \quad (15)$$

On the other hand, discrepancies are found in the formulation of the shear force component due to friction. Three assumptions must be made as discussed by Broere (2001) that concern:

- 1) presence of soil arching effects next to the wedge
- 2) the distribution of vertical effective stress next to the triangular planes of the wedge
- 3) the coefficient of the lateral earth pressure acting on the vertical triangular planes of the wedge

For the first assumption (1), the level of vertical stress next to the wedge is usually assumed to be the same as on the top plane of the wedge (see Eq. (11)). There are two possibilities that exist regarding the distribution of the vertical stress next to the triangular planes of the wedge (2). This results in two possible equations to calculate shear friction force on the triangular plane. In the first possibility, it is assumed that the same stress is present next to the top level of the wedge as next to the vertical plane of the wedge and simultaneously, at the bottom of the wedge, a stress ( $\sigma_{v,bottom}$ ) is present, which solely corresponds to the weight of the soil located along the vertical plane of the wedge. These assumptions are found in Girmscheid (2008), DIN 4126 (2013) and Anagnostou & Kovári (1994). The corresponding distribution of the vertical stress next to the vertical triangular slip surface can be seen in Fig. 23 a). The shear friction force at the triangular side of the wedge is subsequently defined by Eq. (16).

$$T_{R,1} = \tan(\varphi'_2) \cdot K_2 \cdot \left( \frac{D^2 \cdot \sigma_v(t)}{3 \cdot \tan(\vartheta_{crit})} + \frac{D^3 \cdot \gamma_2}{6 \cdot \tan(\vartheta_{crit})} \right) \quad (16)$$

With

$\sigma_v(t)$	Vertical effective stress in tunnel crown [kN/m <sup>2</sup> ]
$K_2$	Coefficient of lateral earth pressure in the wedge area (see Tab. 4) [-]

The second possibility adopts that the vertical stress at the top of the wedge is also equal to the stress next to the wedge. However, in this case, the vertical stress linearly increases along the vertical plane according to the unit weight of present soil (Fig. 23 b). This assumption is found in Kirsch & Kolymbas (2005). The shear friction force is subsequently defined by Eq. (17).

$$T_{R,2} = \tan(\varphi'_2) \cdot K_2 \cdot \left( \frac{D^2 \cdot \sigma_v(t)}{2 \cdot \tan(\vartheta_{crit})} + \frac{D^3 \cdot \gamma_2}{6 \cdot \tan(\vartheta_{crit})} \right) \quad (17)$$

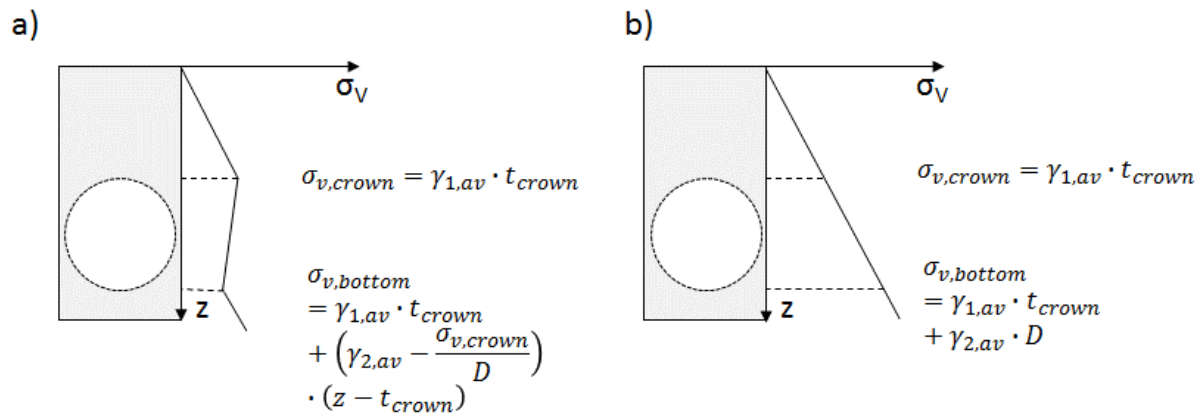


Fig. 23: Two possible distributions of vertical stress next to vertical triangular plane of the wedge: a) Girmscheid (2008), DIN 4126 (2013) and Anagnostou & Kovári (1994) b) Kirsch & Kolymbas (2005)

Authors of this recommendation suggest to use the second variant (Fig. 23b)) based on expected relatively small stress redistribution in the ground due to the shield drive. These particular assumptions for the vertical stress distribution next to the wedge are connected with the coefficients of lateral pressures at the wedge (3). The coefficients are outlined in Tab. 4. The authors of this recommendation suggest to consider  $K_2$  as suggested by Janczecs & Steiner (1994) due to consistency of assumptions regarding the stress redistribution during excavation.

Tab. 4: Suggested coefficients for the lateral earth pressure on the triangular vertical planes of the sliding wedge

Author	Assumed coefficient of the lateral earth pressure
Anagnostou & Kovári (1994)	$K_2 = 0.4$
Jancsecz & Steiner (1994)	$K_2 = \frac{k_0 + k_a}{2}$
Mayer, Hartwig, Schwab (2003)	Shear resistance is neglected
Girmscheid (2008)	$k_a \leq K_2 \leq k_p$
Kirsch & Kolymbas (2005), DIN 4126 (2013)	$K_2 = k_0 = 1 - \sin(\varphi'_2)$

Beside of the support force due to earth pressure, the support force due to the groundwater pressure must also be determined. The groundwater pressure force is easily found by equation (18) assuming that there is no groundwater flow to the tunnel face.

$$W_{re} = \gamma_w \cdot \left( h_{w,crown} + \frac{D}{2} \right) D^2 \quad (18)$$

With

$h_{w,crown}$	Groundwater level above the tunnel crown [m]
$\gamma_w$	Unit weight of water [kN/m <sup>3</sup> ]
D	Tunnel diameter [m]
$W_{re}$	Groundwater pressure force on the rectangular tunnel face area [kN]

Consequently, the obtained forces are recalculated from rectangular wedge face to circular tunnel face and summed after multiplying by the partial safety coefficients (see Eq. (4) in chapter 3).

The required support pressure for the tunnel crown can be calculated based on equation (19). The unit weight of the support medium has to be assumed.

$$s_{crown,min} = \frac{S_{ci}}{\frac{\pi \cdot D^2}{4}} - \gamma_s \cdot \frac{D}{2} \quad (19)$$

With

$\gamma_s$	Unit weight of the support medium [kN/m <sup>3</sup> ]
$s_{crown,min}$	Support pressure in the tunnel crown [kN/m <sup>2</sup> ]

Thus the minimal support pressure is finally defined.

Particularly in German-speaking countries, a limit equilibrium method based on DIN 4085 is sometimes used to calculate the component of support force due to the earth pressure. This method assumes a three-dimensional failure body suggested by Piaskowski & Kowalewski (1965). Three-dimensional active earth pressure acting on the tunnel face is calculated by the help of this failure body (Fig. 24). Note that in case of tunnel face support the angle of wall friction considered in DIN 4085 (Fig. 24) for retaining walls is  $\delta = 0$  deg.

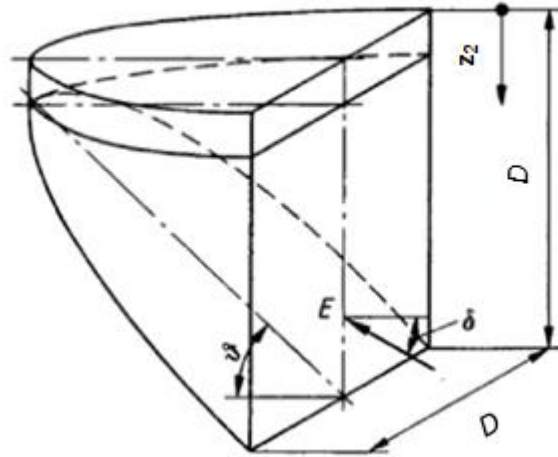


Fig. 24: Failure mechanism acc. to Piaskowski &amp; Kowalewski (1965)

The tunnel face is usually divided into 10 horizontal lamellas for the calculation purposes. For each lamella, the horizontal active earth pressure coefficient is determined based on the friction angle ( $k_{agh}$ ) and cohesion ( $k_{ach}$ ) of the soil within the lamella. Moreover, shape coefficients are calculated for each lamella to take the three-dimensional effect into account (Tab. 5).

Tab. 5: Shape coefficients of the failure mechanism to consider the three dimensional behavior [DIN 4085]

$z_2/D$	0	1	2	3	4	6	8	10
$\mu_{agh} = \mu_{aph} = \mu_{ach}$	1	0.82	0.70	0.59	0.50	0.37	0.30	0.25

With

$\mu_{agh}, \mu_{aph}, \mu_{ach}$	Shape coefficients for earth pressure due to soil friction angle, due to load on the top plane of the failure wedge and due to cohesion [-]
$z_2$	Vertical coordinate starting from the tunnel crown [m]
$D$	Width and height of the failure mechanism, it is equal to the tunnel diameter D [m]

The three-dimensional earth pressure acting on the tunnel face from each lamella is calculated using the following equation:

$$e_{ah,i} = \gamma_i \cdot z_2 \cdot \mu_{agh} \cdot k_{agh,i} + \sigma_{v,crown} \cdot \mu_{aph} \cdot k_{agh,i} - c_i \cdot \mu_{ach} \cdot k_{ach,i} \quad (20)$$

With

$e_{ah,i}$	Earth pressure of particular lamella [kN/m <sup>2</sup> ]
$\gamma_i$	Unit weight of soil [kN/m <sup>3</sup> ]
$z_2$	Vertical coordinate [m]
$\sigma_{v,crown}$	Load on the top plane of the failure wedge (tunnel crown) [kN/m <sup>2</sup> ]
$k_{agh,i}$	Active lateral pressure coefficient due to the friction [-]
$k_{ach,i}$	Active lateral earth pressure coefficient due to the cohesion [-]

The earth pressure resulting from all lamellas is subsequently summarized and multiplied with area of lamellas to obtain the earth pressure force (Eq. 21). The earth pressure force is equal to the support force due to earth pressure (Eq. 4), however, the recalculations for the circular tunnel face is still required. The further calculation approach to obtain the support pressure in the tunnel crown is the same as described for the previous limit equilibrium method.

$$E_{re} = b \cdot \sum_0^D e_{ah,i} \cdot \Delta h \quad (21)$$

With

$E_{re}$  Support force due to earth pressure (rectangular tunnel face) [kN]  
 $\Delta h$  Thickness of a lamella [m]

It is necessary to note that both limit equilibrium approaches deliver a minimum support pressure at which the ground theoretically becomes unstable. It is achieved only due to the application of safety factors that ground deformations are relatively acceptable when obtained support pressure is applied. Since the adopted safety factors are generalized for every soil, the amount of obtained displacement will vary based on the actual stiffness of ground.

## 6.2 Stability ratio method

This method is a practice oriented calculation of support pressure that adopts the stability ratio approach. It considers total parameters of the soil and thus does not separate the support due earth and groundwater pressure. However, the calculated support pressure has to be at least equal to the groundwater pressure (see chapter 5).

The calculation approach is suitable for cohesive ground assuming excavation under undrained conditions. Therefore, a soil with low permeability must be present. Anagnostou & Kovari (1994) states that undrained soil behavior may be expected without further check for shield advance rate higher than 0.1 – 1.0 m/h (1.7 – 16.7 mm/min) and soil permeability lower than  $10^{-7}$  -  $10^{-6}$  m/s. It is necessary to realize that these permeability values were obtained for excavation conditions, therefore during machine stoppage or downtime, a lower ground permeability is required to maintain undrained behavior. This is a very important factor which should not be underestimated. Furthermore, it must be assured that sufficient thickness of soil with undrained behaviour is surrounding the tunnel (Fig. 25).

As a first calculation step, the critical stability ratio has to be adopted for investigated ground conditions, as it expresses the actual stability ratio for which the tunnel face will collapse. The critical stability ratio, depending on considered theory, is usually correlated with the overburden height and with the shield diameter (Tab. 6)

Tab.6: Critical stability ratios from literature;  $t_2$  denotes the overburden thickness of soil with undrained behavior during the excavation ( $t_2$  denotes a thickness of cohesive soil above the shield)

Author	Critical stability ratio
Broms & Bennermark (1967)	$N_{cr} \leq 6$
Davis et al. (1980) – lower bound	$N_{cr} = 4 \cdot \ln\left(2 \cdot \frac{t_2}{D} + 1\right)$
Atkinson & Mair (1981)	$N_{cr} = 5.8613 \cdot \left(\frac{t_2}{D}\right)^{0.4156}$
Casarin & Mair (1981)	$N_{cr} = 3.9254 \cdot \left(\frac{t_2}{D}\right)^{0.36}$

Since the critical stability ratio delivers the support pressure at collapse, a required safety margin must be included in the calculation. The assumed safety margin is determining the actual existing stability ratio (Eq. (22)). The generally accepted correlations between soil behaviour on the tunnel face and actual stability ratios are outlined in Tab. 7.

$$N = \frac{N_{cr}}{\eta} \quad (22)$$

With

$N$  Existing stability ratio [-]  
 $\eta$  Safety factor (here  $\eta = 1.5$ ) [-]

Tab. 7: Generally accepted stability ratios and the consequences for the tunnel face stability [Leca & New, 2007]

Tunnel face behavior	Stability ratio
The overall stability of the tunnel face is usually ensured	$N < 3$
Special consideration must be taken of the evaluation of the settlement risk	$3 < N < 5$
Large amounts of ground losses being expected to occur at the face	$5 < N < 6$
Tunnel face instable, collapse may occur	$N > 6$

Consequently, the required support pressure at the tunnel axis can be determined by Eq. (23)

$$s_{axis} = \sigma_{v,tot,axis} - N \cdot c_u \quad (23)$$

With

N	Existing stability ratio [-]
$\sigma_{v,tot,axis}$	Total stress at the tunnel axis (surcharge on the surface is to be included here) [kN/m <sup>2</sup> ]
$s_{axis}$	Support pressure at the tunnel axis [kN/m <sup>2</sup> ]
$c_u$	Undrained shear strength of the soil [kN/m <sup>2</sup> ]

Given  $s_{axis}$ , the required support pressure for the tunnel crown can be calculated (Eq. (24)). The unit weight of the support medium has to be assumed.

$$s_{crown,min} = s_{axis} - \gamma_s \cdot \frac{D}{2} \quad (24)$$

With

$\gamma_s$	Unit weight of the support medium [kN/m <sup>3</sup> ]
$s_{crown,min}$	Support pressure in the tunnel crown [kN/m <sup>2</sup> ]

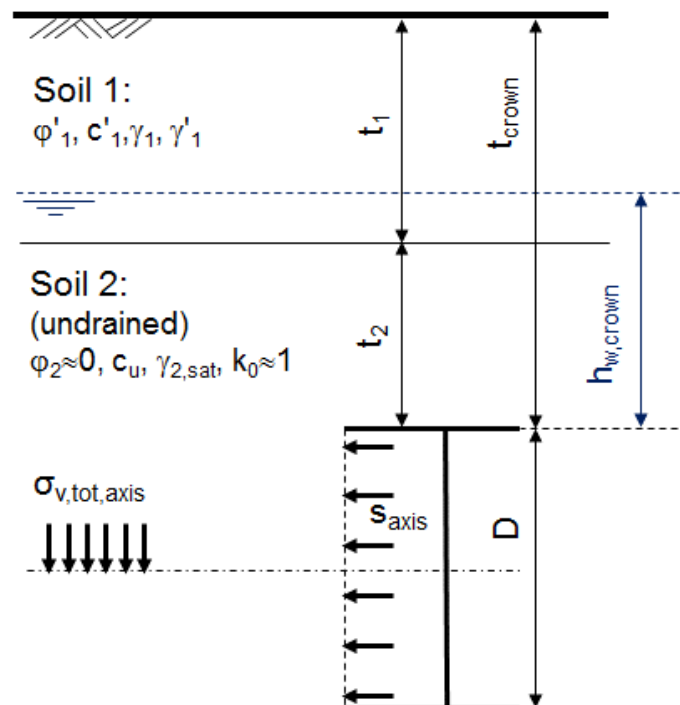


Fig. 25: Model layout of the stability ratio method

For the input of equation (23), the total vertical stress at the tunnel axis has to be determined. This is done based on equation (25). CAUTION: For excavations in overconsolidated ground with horizontal

total stress larger than vertical, it is recommended to consider the higher one as  $\sigma_{v,tot,axis}$  due to safety reasons (for more information, see Davis et al. (1980)).

$$\sigma_{v,tot,axis} = \sigma_{v,interface} + (t_2 + 0.5 \cdot D) \cdot \gamma_{2,sat} \quad (25)$$

With

$\sigma_{v,tot,axis}$	Total stress at tunnel axis [kN/m <sup>2</sup> ]
$\sigma_{v,interface}$	Total vertical stress at the interface between soil 1 (drained) and soil 2 (undrained). This also includes the surcharge on the surface [kN/m <sup>2</sup> ]
$t_2$	Thickness of soil with undrained behavior above the tunnel crown [m]
$D$	Shield diameter [m]
$\gamma_{2,sat}$	Saturated unit weight of soil 2 [kN/m <sup>3</sup> ]

In the case of compressed-air interventions, it is recommended to check the local failure (Fig. 26) mode with equation (26) by Davis et al. (1980). This check is particularly important, if a large shield diameter is employed and soil with low undrained cohesion may be encountered. Equation (26) was derived for a circular tunnel heading adopting the upper bound theorem (section 4.1). For further details, see Li et al. (2009).

$$\frac{\gamma_{2,sat} \cdot D}{c_u} \leq 10.96 \quad (26)$$

If the calculated value is greater than 10.96, it is only recommended to partially lower the support medium in the excavation chamber (e.g. half compressed air and half EPB or slurry support).

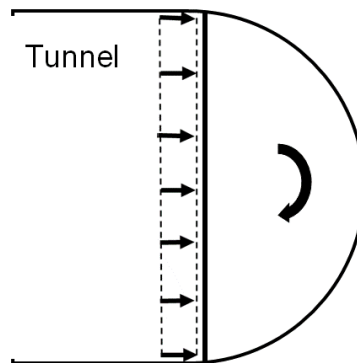


Fig. 26: Local failure mode of the compressed air supported tunnel face

### 6.3 Numerical methods

For special cases such as excavation close to sensitive surface constructions, the amount of support pressure has to be defined based on admissible surface settlements. In these scenarios, the “Serviceability Limit State Approach” is adopted (section 2.1). Hence, machine – ground interaction is investigated.

Numerical methods based on the finite element approach, are applied in practice to analyse machine-ground interactions. The most favourable method used to determine the relationship between applied face pressure and obtained surface settlement is the full 3D step-by-step analysis with consideration to the progress of the shield machine. Besides face pressure, this analysis also assesses the influence of tail void grouting pressure. However, the definition of optimal face support pressure based on the full 3D analysis is extremely time consuming as multiple 3D FEM simulations are required.

Therefore, a quicker, simplified 2D plane strain approach has gained popularity in practice (excavation perpendicular to the model slice). In this method, support pressure is applied on the 2D cavity boundary. The relationship between applied pressure and ground deformations is observed. Unfortunately, it is not possible to state if this simplified 2D analysis is more or less safe compared to a real scenario without performing a full 3D simulation.

An intermediate step between full 3D and plain strain 2D analysis is known as “pseudo 3D analysis”. The key distinction between pseudo 3D analysis and full 3D step-by-step analysis is that the step-by-step drive of the shield machine is not taken into account in a pseudo 3D analysis. The 3D stress state is still preserved. This type of analysis is beneficial in comparison to 2D, if a shield drive under surface construction with small length is assessed.

### 6.4 Summary

The calculated support pressures exhibit relatively wide scattering in non-cohesive soils depending on the adopted formulation of the limit equilibrium approach (for reference, see Vu et al. (2015) or Kirsch (2010)). In cohesive-frictional soils, the size of calculation scattering will decrease. It is recommended to ensure that any assumptions used to calculate variables in limit equilibrium methods are consistent with regard to the adopted mobilization of soil’s shear resistance.

The assumptions for the stability ratio method about critical stability ratio and amount of undrained soil cohesion are key factors that determine the results. The critical stability ratio should be adopted based on a case by case basis and local experience. Furthermore, the amount of undrained cohesion should be conservatively assessed. Nevertheless, the critical stability ratio method often shows the acting groundwater pressure as the decisive factor for support pressure calculations.

When designing the support pressure for excavation in the particular ground conditions, it is necessary to consider the extent of possible consequences such as failures or settlements, due to an inappropriate design. The extent of the worst case scenario determines how conservative the calculation approach should be. A general rule of thumb is that inappropriate support pressure may lead to immediate failure up to the surface for a combination of slurry shields and non-cohesive ground. With a combination of EPB shields and cohesive soil, it may lead “only” to extensive surface deformations without failure up to the surface. The height of the overburden plays a significant role for the extent of consequences.

For excavations in difficult ground conditions, e. g. in complicated weak ground or under surface constructions, it is recommended that the analytical calculation of the support pressure should always be supplemented by the analysis of machine – ground interaction.

## 7 Additional aspects to be considered in the analysis

### 7.1 Support pressure deviations

Support pressure deviations must be considered in calculations, which are performed according to ZTV- ING (2012) - see chapter 3:

- +/- 10 kN/m<sup>2</sup> for slurry shield and for compressed-air support mode of both shield types
- +/- 30 kN/m<sup>2</sup> for EPB shield

For the EPB shield, the range of deviation was defined to be larger because of a higher degree of uncertainty for the support pressure regulation. The deviations are added to the lower support pressure limit and subtracted from the upper pressure limit (compare Fig. 9). However, the large range of deviations for an EPB shield may in some cases lead to a limited feasibility of EPB shield drives. Thus, EPB shield deviations may be reduced for special cases upon proper justification. Reduction of the range should focus especially on the deviations at the upper pressure limit, since the risk of overburden break-up or support medium blow-out in the case of EPB is relatively low. A good shield operation, process controlling and good design of excavation process (e.g. soil conditioning) are fundamentally required for such a reduction.

### 7.2 Heterogeneous tunnel face in layered soft ground

A tunnel face in a layered soft ground can be heterogeneous from two viewpoints. One part of the tunnel face could show drained behaviour while another part could show undrained. From this perspective, the conditions for the whole tunnel face should be viewed as drained and a limit equilibrium method should be used for calculation.

In the second viewpoint, the soil behaviour on the tunnel face consistently is either drained or undrained. However, the shear strength properties of soils at the tunnel face could be strongly diverging. Both the limit equilibrium and the stability ratio method assume a homogeneous tunnel face<sup>1</sup>. Therefore, soils on the tunnel face are usually homogenised in practice-oriented calculations. A more precise limit equilibrium method for the heterogeneous tunnel face was suggested by Broere (1999). The method is based on the horizontal slices method which was developed by Walz (1983) to calculate stability of a diaphragm wall trench. Broere (1999) formulated the equilibrium on infinitesimally small horizontal slices of the wedge. There was no possible consideration of different sliding angles for layers with different shear properties in the model and used a global sliding angle for all layers instead. The global sliding angle for the heterogeneous face had to be calculated with the help of numerical methods. The numerical calculations performed by Zizka et al. (2013) showed that determining a uniform sliding angle for heterogeneous tunnel faces is extremely complicated to find for some cases. This aspect, in addition to the complex equations defining the equilibrium on the wedge, caused that the approach did not succeed widely in practice.

Due to previously mentioned factors, the weighted average approach for homogenization of the tunnel face is often employed in practice. Two additional calculations considering the best case and the worst case scenario should complement the calculation. The worst case scenario plays a more critical role and assumes the whole tunnel face consists of soil showing the worst shear properties among the heterogeneous tunnel face. In contrast, the best case scenario calculates the required face pressure for ground conditions consisting of soil from heterogeneous tunnel face characterized by the best

---

<sup>1</sup> The calculation method after DIN 4085 allows the consideration of heterogeneous tunnel face, however, the calculation has to be performed with caution for a tunnel face consisting from soils with highly different shear properties.

shear properties. The minimal support pressure for the excavation should be adopted between these two borders based on engineering judgement.

### 7.3 Mixed tunnel face with rock and soil

A simultaneous presence of hard rock and soft soil is defined as “mixed face” for the purpose of this recommendation. Several operational problems are connected with tunnel excavations in mixed tunnel faces [Thewes, 2004]. Several case scenarios should be considered for mixed ground conditions regarding the tunnel face stability assessment and the determination of the support pressure.

In case 1 (Fig. 27), excavation is performed with an EPB shield and the tunnel face consists mostly of soft soil material with only a small portion of hard rock. The calculation of support pressure should be carried out with the assumption that the whole tunnel face consists of soft soil. During excavation, EPB face support can be maintained since the majority of material in the excavation chamber contains from soft soil with the required properties (see section 2.4.2.). However, there is a considerable risk that the rock cutting tools (disc cutters) may be overloaded while cutting the small rock layer. It will be very difficult for a shield driver to limit the contact force of the disc cutter to the allowable force, particularly when operating in EPB mode with a large penetration (mm/rev.). Penetration must be here limited to an allowable value based on the expected rock strength.

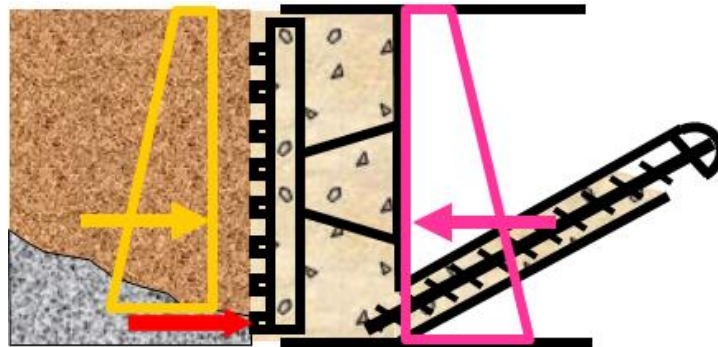


Fig. 27: Case 1- EPB with a smaller area of the tunnel face in hard rock, yellow arrow – Earth pressure force, red arrow – cutting tools loading while passing through hard rock area with possible overloading

In case 2 (Fig. 28), the EPB shield must progress through a mixed tunnel face composed mostly of hard rock and just a small fraction of soil. The support pressure calculations would be carried out the same way as for soft soil areas except with an adopted surrogate tunnel diameter which corresponds to the thickness of the present soft soil. For an EPB, however, this support pressure would be difficult to maintain because the cuttings in the chamber consisting by majority of hard rock chips. These rock chips do not allow for a low permeability EPB muck with necessary flow characteristics. Resulting problems may be:

- Uncontrolled groundwater inflow into the excavation chamber
- Insufficient face support of the soft ground section of the tunnel face
- Excessive wear of tools, cutting wheel structure and other components
- Excessive heat development which leads to required cooling periods during excavations for main bearing sealing system and before man access for interventions during stoppages
- Problems to keep face stability under compressed air for inspection, maintenance and repair

This situation may be partially improved by extensive injections of conditioning agents into the excavation chamber, which particularly should aim to reducing permeability and abrasivity of the earth muck.

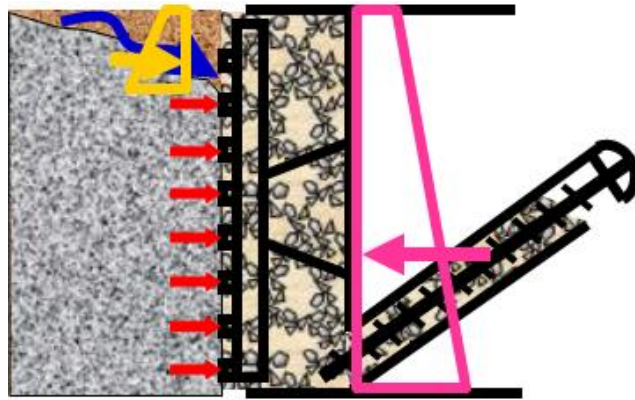


Fig. 28: Case 2 – EPB with larger area of the tunnel face in hard rock formation, yellow arrow – Earth pressure force, red arrow – cutting tools loading while passing through hard rock

In case 3 (Fig. 29), a slurry shield excavates through mixed face conditions. The calculation of support pressure would be carried out for the soft soil section while adopting a corresponding surrogate excavation diameter. This support pressure can easily be maintained for any composition of mixed face tunnel face.

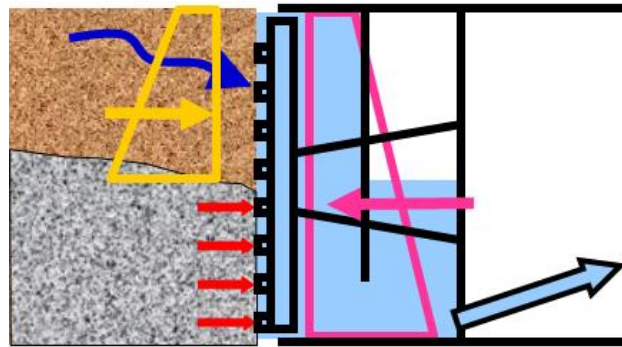


Fig. 29: Case 3 – Slurry shield for all compositions of mixed face, yellow arrow – Earth pressure force, red arrow – cutting tools loading while passing through hard rock

#### 7.4 Excess pore pressure during excavation with a slurry shield

During slurry shield excavations in saturated sandy soil, excess pore pressure may form in front of the tunnel face due to the slurry filtration process. This excess pore pressure may subsequently leads to a reduction of the safety factor adopted in the face stability calculation. Currently, there are no generally performed approaches in tunnelling practice to calculate the amount of excess pressure. Some theoretical approaches have been discussed by Bezuijen et al. (2001) and Broere & van Tol (2000). Fig. 30 shows a case that incorporates the excess pore pressure in the face stability calculation according the method outlined by Jancsecz & Steiner (1994).

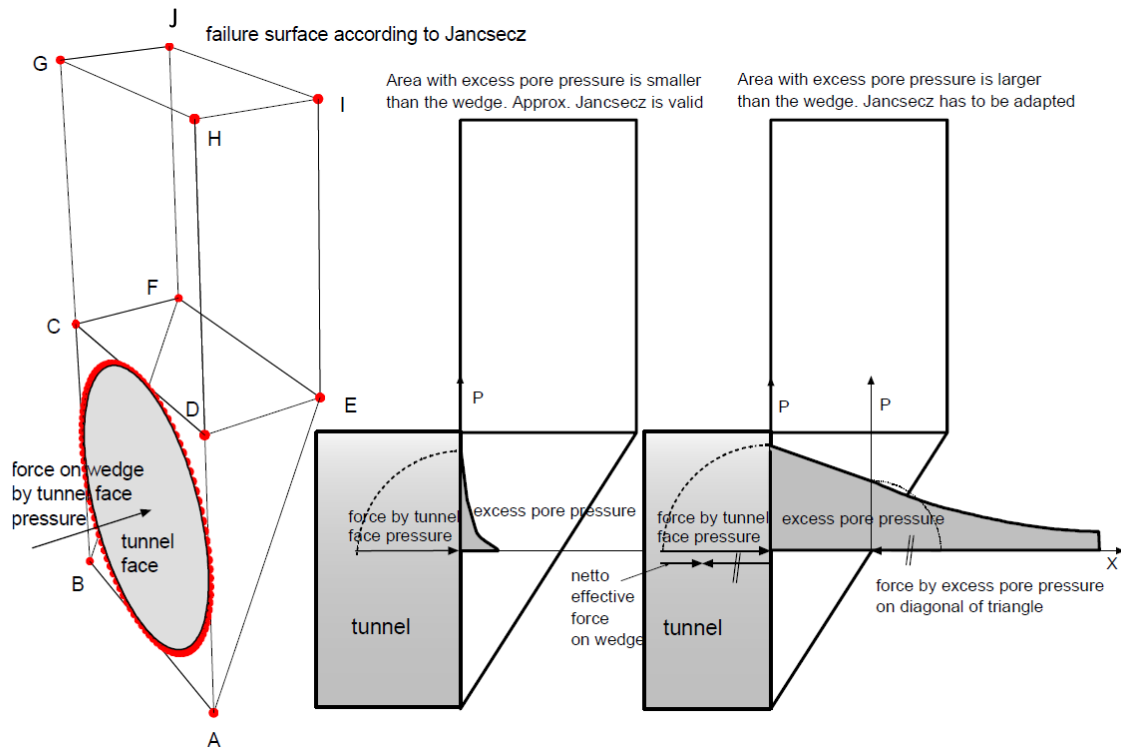


Fig. 30: Excess support pressure in front of the tunnel face [Bezuijen et al, 2001]

The amount of excess pore pressure can be measured by pore water pressure sensors during excavation. Such measurements have been performed during the construction of the 2<sup>nd</sup> Heineoord tunnel [Bezuijen et al, 2001]. This allows for subsequent countermeasures based on measured excess pore pressure e.g.: adjustment of support pressure, adjustment of slurry properties.

## 8 Calculation examples

### 8.1 Coarse ground

- Excavation within a coarse sandy soil using a slurry shield
- Typical calculations using Horn's failure mechanism and ZTV-ING safety concept (chapter 3)
- Calculation for two different grain size distribution

The excavation, deploying a slurry shield, is planned in a sandy soil (Tab. 8). The tunnel diameter is 10 m and the overburden height is 15 m. Groundwater level is 2 m below the surface. The required support pressure for the excavation is calculated using the ultimate limit state approach. The calculation is performed under drained conditions. The calculation will be done for two cases. In Case 1, the sandy soil has a characteristic grain size  $d_{10}=0.15$  mm. In Case 2, the sandy soil has a characteristic grain size  $d_{10}=0.80$  mm. The aim of these two investigations is to show the influence of soil grain size on the required support pressure in slurry shield excavations. All other soil properties are assumed to remain constant in both cases.

Tab.8: Input parameters of the sandy soil

	$\phi'$ [°]	$c'$ [kN/m <sup>2</sup> ]	$\gamma$ [kN/m <sup>3</sup> ]	$\gamma'$ [kN/m <sup>3</sup> ]	$\gamma$ min [kN/m <sup>3</sup> ]	$\gamma'$ min [kN/m <sup>3</sup> ]	$d_{10}$ Case 1 / Case 2 [mm]
Sandy soil	30	0	18	8	17	7	0.15 / 0.80

#### 8.1.1 Case 1 – membrane pressure transfer model

The characteristic grain size of the sandy soil is  $d_{10}=0.15$  mm. A bentonite slurry with a yield point  $\tau_f = 30$  N/m<sup>2</sup> will be used for excavation. This slurry fulfils the requirement for the minimal yield point that assure the local stability described in section 2.4.1 Eq. (3). The pressure gradient after Eq. (1) for this ground and slurry combination is 700 kN/m<sup>3</sup> (higher than 200 kN/m<sup>3</sup>) thus the support pressure will be transferred by a filter cake (membrane) on the tunnel face (compare section 2.3.3). Therefore, it is assumed that the full amount of the slurry pressure will efficiently support the tunnel face.

#### 1. Machine Parameters

$D = 10$ m	Shield diameter
$\Delta = 10$ kN/m <sup>2</sup>	Support pressure deviations (+/-)
$\gamma_s = 12$ $\frac{kN}{m^3}$	Unit weight of support medium, regular advance

#### 2. Safety factors chosen for calculations

$\eta_E = 1.5$	Earth pressure safety factor
$\eta_W = 1.05$	Water pressure safety factor
$\Delta_W = 10$ kN/m <sup>2</sup>	Minimal support – overpressure to water pressure
$\sigma_s = 10$ kN/m <sup>2</sup>	Traffic load at surface

### 3. Calculation approach

- a). **Input in equation (8) describing limit equilibrium on the wedge. Note, the sliding angle is not yet known.**

Earth pressure force according to Equation (8):

$$E_{re}(\vartheta) = \frac{(G + P_v) \cdot (\sin(\vartheta) - \cos(\vartheta) \cdot \tan(\varphi'_2)) - 2 \cdot T - c'_2 \cdot \frac{D^2}{\sin(\vartheta)}}{\sin(\vartheta) \cdot \tan(\varphi'_2) + \cos(\vartheta)}$$

Friction force on the triangular vertical plane of the sliding wedge, see Eq. (17):

$$T_R = K_2 \cdot \tan(\varphi'_2) \cdot \left( \frac{D^2 \cdot \sigma_v(t_{crown})}{2 \cdot \tan(\vartheta_{crit})} + \frac{D^3 \cdot \gamma_{2,av}}{6 \cdot \tan(\vartheta_{crit})} \right)$$

Lateral pressure coefficient to be considered in  $T_R$ :

$$K_2 = \frac{k_0 + k_a}{2} = \frac{\tan\left(45 - \frac{\varphi'_2}{2}\right)^2 + 1 - \sin(\varphi'_2)}{2} = 0.417$$

Self-weight of the sliding wedge, see Eq. (10):

$$G = \frac{1}{2} \cdot \frac{D^3}{\tan(\vartheta_{crit})} \cdot \gamma_{2,av}$$

Vertical force on the wedge, silo-theory is not considered, see Eq. (13):

$$P_v = \frac{D^2(\gamma_{1,av} \cdot t_{crown} + \sigma_0)}{\tan(\vartheta_{crit})}$$

- b). **Maximization of support force due to the earth pressure using the variation of sliding angle.**

Resulting sliding angle for  $E_{max,re}$ :

$$\vartheta_{crit} = 66.56 \text{ deg}$$

- c). **Determination of forces**

Values based on resulting sliding angle **b)** :

$$T_R(\vartheta_{crit}) = 921.3 \text{ kN}$$

$$G(\vartheta_{crit}) = 1734.3 \text{ kN}$$

$$P_v(\vartheta_{crit}) = 6503.7 \text{ kN}$$

Maximal required support force due to earth pressure, Eq. (8):

$$E(\vartheta_{crit}) = 4122.32 \text{ kN}$$

Recalculation of the force determined from rectangular-shaped front plane of the wedge to the real circular tunnel face:

$$E_{max,ci} = E_{re}(\vartheta_{crit}) \cdot \frac{\pi D^2}{4} = 3237.7 \text{ kN}$$

Acting water pressure force on the rectangular tunnel face, see Eq. (18):

$$W_{re} = \gamma_w \cdot \left( h_{w,crown} + \frac{D}{2} \right) D^2$$

Acting water pressure force on the circular tunnel face, see Eq. (18):

$$W_{ci} = W_{re} \cdot \frac{\pi D^2}{4} = 14137.2 \text{ kN}$$

Total support force considering safety factors, see Eq. (4):

$$S_{ci} = \eta_E \cdot E_{max,ci} + \eta_W \cdot W_{ci} = 19700.5 \text{ kN}$$

Support force to counter earth pressure considering safety coefficient:

$$S_{E,ci} = \eta_E \cdot E_{max,ci} = 4856.5 \text{ kN}$$

Support force to counter water pressure considering safety coefficient:

$$S_{W,ci} = \eta_W \cdot W_{max,ci} = 14843.9 \text{ kN}$$

#### d). Determination of pressures and checks

Minimal support pressure for the tunnel crown, see Eq. (19):

$$s_{crown,min} = \frac{S_{ci}}{\pi \cdot D^2} - \gamma_s \cdot \frac{D}{2} = 190.8 \text{ kN/m}^2$$

The support pressure  $s_{crown,min}$  must be  $\eta=1.05$  times higher than groundwater pressure in the tunnel crown (in the case of support medium lowering and compressed air intervention, this check has to be fulfilled for the lowest point of the compressed air support at the tunnel face – see chapter 3):

$$1.05 \cdot w_{crown} = 1.05 \cdot \gamma_w \cdot h_{w,crown} = 136.5 \frac{\text{kN}}{\text{m}^2} < s_{crown,min} = 190.8 \text{ kN/m}^2$$

Support pressure at the tunnel crown for regular advance with consideration of support pressure deviations +/- 10 kN/m<sup>2</sup> (see section 7.1):

$$s_{crown,advance,min} = s_{crown,min} + 10 \text{ kPa} = 200.8 \text{ kN/m}^2$$

Total stress at tunnel crown with consideration if the minimal unit weight of the soil:

$$\sigma_{v,crown,min} = \gamma_{1,av,min} \cdot t_{crown} + w_{crown} = 255 \text{ kN/m}^2$$

Maximal allowable support pressure at tunnel crown due to break-up safety:

$$s_{crown,max} = 0.9 \cdot \sigma_{v,crown,min} = 229.5 \text{ kN/m}^2$$

Highest support pressure due to face pressure deviations:

$$s_{crown,advance,max} = s_{crown,max} - 10 \text{ kPa} = 219.5 \text{ kN/m}^2$$

Compare value with  $s_{crown,advance,min}$ . If  $s_{crown,advance,max}$  is higher than  $s_{crown,advance,min}$ , the excavation is possible.

#### 4. Conclusion

The excavation should be performed with support pressures between 201 kN/m<sup>2</sup> and 219 kN/m<sup>2</sup> (support pressure deviations are included) set at the tunnel crown (Fig. 31). Calculations were performed with the assumption of filter cake formation on the tunnel face. Hence, complete amount of the slurry pressure is transferred on the tunnel face. This was proven by the analysis of slurry ground interaction described in section 2.4.1. In case of a deep slurry penetration into the soil skeleton, the required support pressure would have to be increased following DIN 4126 (2013) or Anagnostou & Kovari (1994), as it is demonstrated in the following sub-chapter.

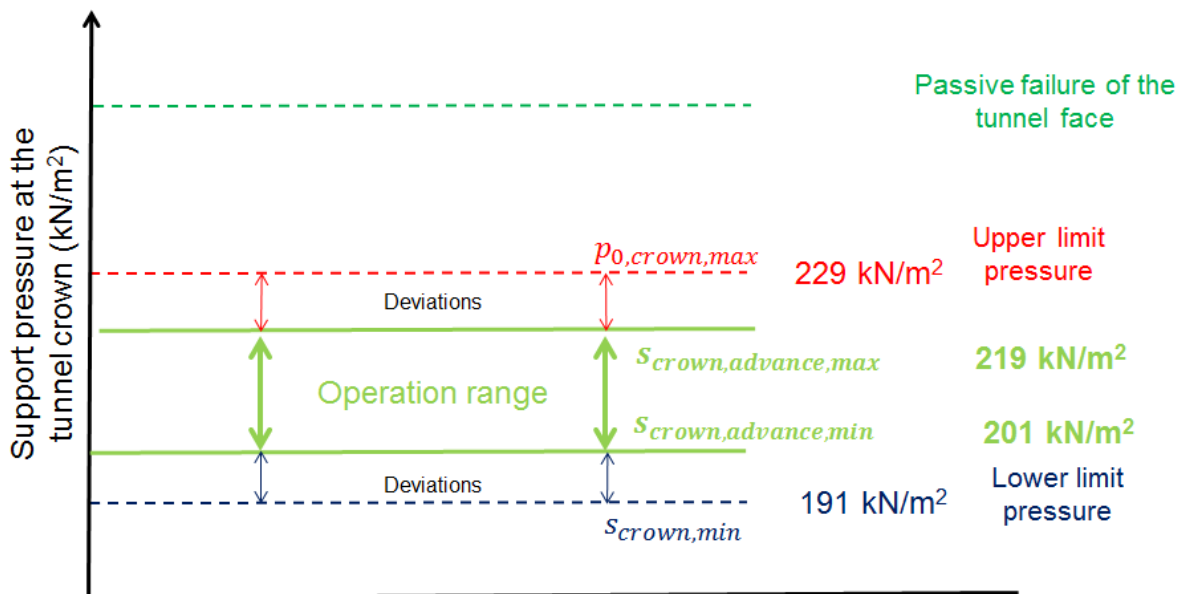


Fig. 31: Support pressure limits at the tunnel crown of Case 1, excavation in sandy soils

#### 8.1.2 Case 2 – penetration pressure transfer model

The characteristic grain size of the sandy soil is in this case  $d_{10} = 0.8$  mm. A bentonite slurry with a yield point  $T_f = 30$  N/m<sup>2</sup> will be used for excavation. The slurry fulfils the minimal yield point that assures local stability described in section 2.4.1 Eq. (1).

$$f_{so} = \frac{3.5 \cdot 0.03}{0.0008} = 131 \text{ kN/m}^3$$

The pressure gradient after Eq. (1) for this ground and slurry combination is 131 kN/m<sup>3</sup> (lower than 200 kN/m<sup>3</sup>) thus the support pressure will be transferred by a penetration zone on the tunnel face (see section 2.3.3). Thus only a reduced amount of slurry pressure will be transferred onto the soil skeleton within the wedge, accordingly to Fig. 8.2. The amount of support force and pressure efficiently stabilizing the tunnel face will be investigated within this section.

The calculation approach for the support force and for the support pressure would be performed in the same manner as case 1 (section 8.1.1). The following values have been already obtained from case 1:

- Required total support force considering safety factors:  $S_{ci} = 19700 \text{ kN}$
- Minimal support pressure for the tunnel crown:  $S_{crown,min} = 190.8 \text{ kN/m}^2$
- Minimal support pressure for the tunnel axis:  $S_{axis,min} = 250.8 \text{ kN/m}^2$
- Minimal support pressure for the tunnel invert:  $S_{invert,min} = 310.8 \text{ kN/m}^2$

Subsequently, the actual transferred pressure will be obtained according to the approach of Anagnostou & Kovari (1994).

1. Excess slurry pressure  $\Delta p$  (= groundwater pressure subtracted from the slurry pressure at particular elevation of the tunnel face, compare Eq. 2)

- Tunnel crown  $\Delta p_c = 60.8 \text{ kN/m}^2$
- Tunnel axis  $\Delta p_a = 70.8 \text{ kN/m}^2$
- Tunnel invert  $\Delta p_i = 80.8 \text{ kN/m}^2$

2. Penetration distance of the slurry ( $e_{max}$ ) by rearranging Eq. (2) using the corresponding  $\Delta p_n$

- Tunnel crown  $e_{max,c} = 0.464 \text{ m}$
- Tunnel axis  $e_{max,a} = 0.541 \text{ m}$
- Tunnel invert  $e_{max,i} = 0.617 \text{ m}$

3. Comparison of the slurry penetration distance and the dimensions of the sliding soil wedge which must be stabilized by the slurry (Fig. 32).

- Length  $b$  of the wedge (silo) considering  $\vartheta_{crit} = 66.56 \text{ deg}$   $b = 4.34 \text{ m}$
- Coordinate  $x$   $x = 1.372 \text{ m}$
- Slurry excess pressure at distance  $x$  from invert  $\Delta p_x = 78.1 \text{ kN/m}^2$
- Penetration distance at distance  $x$  from invert  $e_{max,x} = 0.600 \text{ m}$
- Area AA (area with the red border in Fig. 32 b)  $AA = 5.002 \text{ m}^2$
- Area BB (blue area in Fig. 32)  $BB = 5.405 \text{ m}^2$
- Ratio AA/BB  $AA/BB = 92 \%$

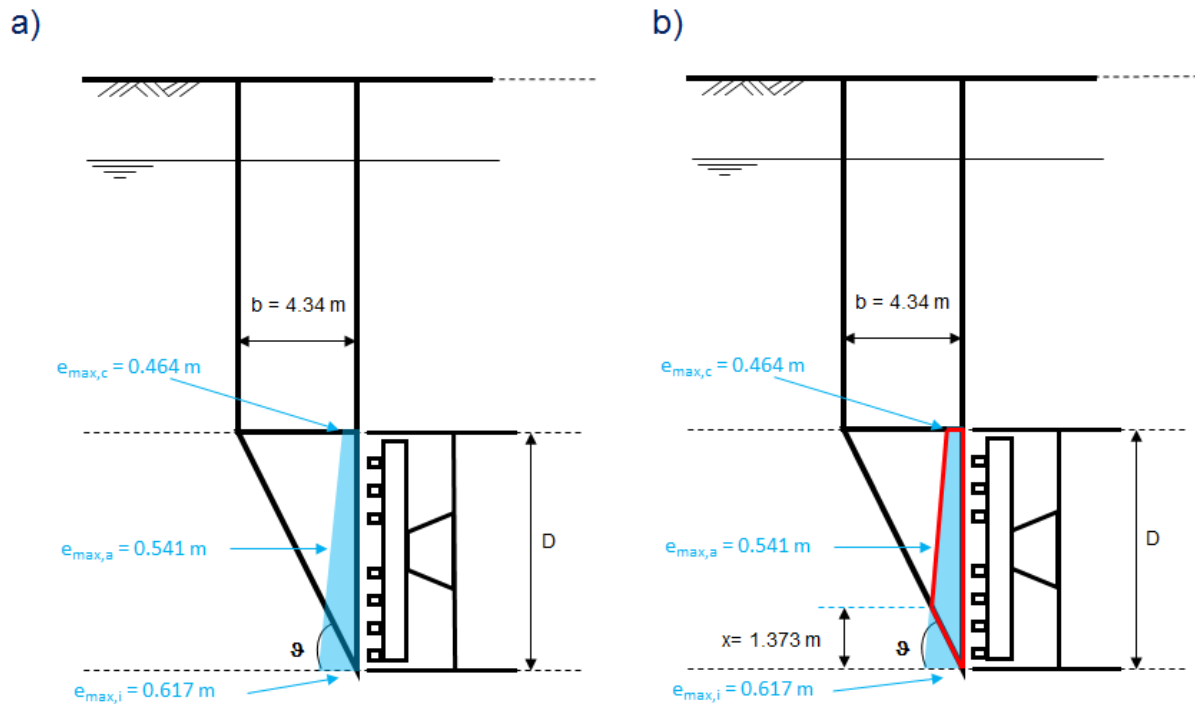


Fig. 32: Slurry penetration in front of the tunnel face: a) shows the maximal penetration distances of the slurry. In b), the area with red border signifies a penetration zone where the slurry pressure is efficiently supporting the sliding wedge

#### 4. Determination of the total support force transferred

- Support force required to counter earth pressure  $S_{E,ci} = 4856.5 \text{ kN}$
- Support force required to counter water pressure  $S_{W,ci} = 14843.9 \text{ kN}$
- Support force transferred to efficiently counter earth pressure:

$$S_{E,trans,ci} = S_{E,ci} \cdot \frac{AA}{BB} = 4856.5 \text{ kN} \cdot 92\% = 4468.0 \text{ kN}$$

- Total support force transferred:

$$S_{total,trans,ci} = S_{E,trans,ci} + S_{W,ci} = 19311.9 \text{ kN}$$

- Efficiency of the pressure transfer

$$Efficiency = \frac{S_{total,transf}}{S_{total,req}} = 0.98$$

#### 5. Conclusion

Due to the penetration of slurry into the ground, only 98 % of the slurry support force will be efficiently used to support the tunnel face.

The approach described above must be repeated for a chosen higher slurry pressure until the transfer efficiency is greater than 1. This iterative approach is required, as a higher slurry pressure induces a higher penetration distance of the slurry. Also, the yield point of the slurry could be increased, which would lead to a reduced penetration distance of the slurry.

## 8.2 Cohesive ground

- Excavation with an EPB shield within cohesive soft soil under undrained conditions
- Cohesive ground – a stability ratio approach and ZTV-ING safety concepts (chapter 3)

The excavation, deploying an EPB shield, is planned in a clayey soil (Tab. 9) covered by a sandy soil. The tunnel diameter is 10 m and the overburden height of clayey soil is 13 m covered by 2 m of a sandy soil. Groundwater level is located 2 m below the surface. The required support pressure for the excavation has to be defined using the ultimate limit state approach. The clayey soil can be characterized with low permeability. The distance between the tunnel crown and the upper edge of the clayey soil is sufficiently high (13 m). Therefore, undrained conditions may be assumed for the excavation. The cohesion mentioned in Tab. 9 for clayey soil denotes the undrained cohesion ( $c_u$ ). It is assumed that the groundwater pressure is compensated by the support pressure. Thus, no seepage forces have to be investigated.

Tab.9: Input parameters of the sandy and clayey soil

	$\varphi$ [°]	$c_u$ [kN/m <sup>2</sup> ]	$\gamma$ [kN/m <sup>3</sup> ]	$\gamma'$ [kN/m <sup>3</sup> ]	$\gamma$ min [kN/m <sup>3</sup> ]	$\gamma'$ min [kN/m <sup>3</sup> ]
Clayey soil	0	40	19	9	18	8
Sandy soil	30	0	18	8	17	7

### 1. Machine Parameters

$D = 10 \text{ m}$	Shield diameter
$\Delta = 30 \text{ kN/m}^2$	Support pressure deviations (+/-)
$\gamma_s = 14 \frac{\text{kN}}{\text{m}^3}$	Density of support medium, regular advance

### 2. Safety factors chosen for calculations

$\eta_E = 1.5$	Earth pressure safety factor
$\eta_W = 1.05$	Water pressure safety factor
$N_{cr} = 6.537$	Critical stability ratio for the investigated excavation, based on Atkinson & Mair (1981), see Tab. 6
$N \cong 4.358$	Adopted stability ratio for the calculation, see Eq. (22)
$\sigma_s = 10 \text{ kN/m}^2$	Traffic load at surface

### 3. Calculation approach

#### a). Total vertical stress at the interface between cohesionless and cohesive soil

$$\sigma_{v,interface} = (\sigma_0 + \gamma_{sand} \cdot t_1) + 0 = 10 + 18 \cdot 2 = 46 \text{ kN/m}^2$$

**b). Total vertical stress at the elevation of the tunnel axis**

$$\sigma_{v,axis} = \left( t_{crown} + \frac{D}{2} \right) \cdot \gamma_{clay} + \sigma_{v,interface} = \left( 13 + \frac{10}{2} \right) \cdot 19 + 46 = 388 \text{ kN/m}^2$$

**c). Support pressure at the elevation of the tunnel axis**

$$s_{axis} = \sigma_{v,axis} - N \cdot c_u = 388 - 4.358 \cdot 40 = 213.7 \text{ kN/m}^2 \quad \text{see Eq. (23)}$$

Water pressure at the tunnel axis:

$$w_{axis} = 180 \text{ kN/m}^2$$

If the groundwater pressure is lower than the acting earth pressure, the earth pressure is used for further calculations:

$$\eta_w \cdot w_{axis} = 189 \text{ kN/m}^2$$

**d). Required support pressure at the tunnel crown**

Minimal support pressure for the tunnel crown, see Eq. (4):

$$s_{crown,min} = s_{axis} - \gamma_s \cdot \frac{D}{2} = 143.7 \text{ kN/m}^2$$

The support pressure  $s_{crown,min}$  must be 1.05 times higher than groundwater pressure in the tunnel crown (in the case of support medium lowering and compressed air intervention, this check has to be fulfilled for the lowest point of the compressed air support at the tunnel face – see chapter 3):

$$1.05 \cdot w_{crown} = 1.05 \cdot \gamma_w \cdot h_w = 136.5 \frac{\text{kN}}{\text{m}^2} < s_{crown,min} = 143.7 \text{ kN/m}^2$$

Support pressure at the tunnel crown for regular advance with consideration of support pressure deviations +/- 30 kN/m<sup>2</sup>:

$$s_{crown,advance,min} = s_{crown,min} + 30 \text{ kN/m}^2 = 173.7 \text{ kN/m}^2$$

Total stress at tunnel crown with consideration of the minimal unit weight of the soils:

$$\sigma_{v,crown,min} = \gamma_{sand,min} \cdot h_1 + \gamma_{clay,min} \cdot h_2 = 268 \text{ kN/m}^2$$

Maximal allowable support pressure at tunnel crown due to break-up safety:

$$s_{crown,max} = 0.9 \cdot \sigma_{v,crown,min} = 241.2 \text{ kN/m}^2$$

Highest support pressure due to face pressure deviations for regular advance:

$$s_{crown,advance,max} = s_{crown,max} - 30 \text{ kN/m}^2 = 211.2 \text{ kN/m}^2$$

Compare this value with  $s_{crown,advance,min}$ . If  $s_{crown,advance,max}$  is higher than  $s_{crown,advance,min}$ , the excavation is possible.

**4. Conclusion**

The excavation should be run with support pressures between 174 kN/m<sup>2</sup> and 211 kN/m<sup>2</sup> (support pressure deviations are included) set at the tunnel crown (Fig. 33).

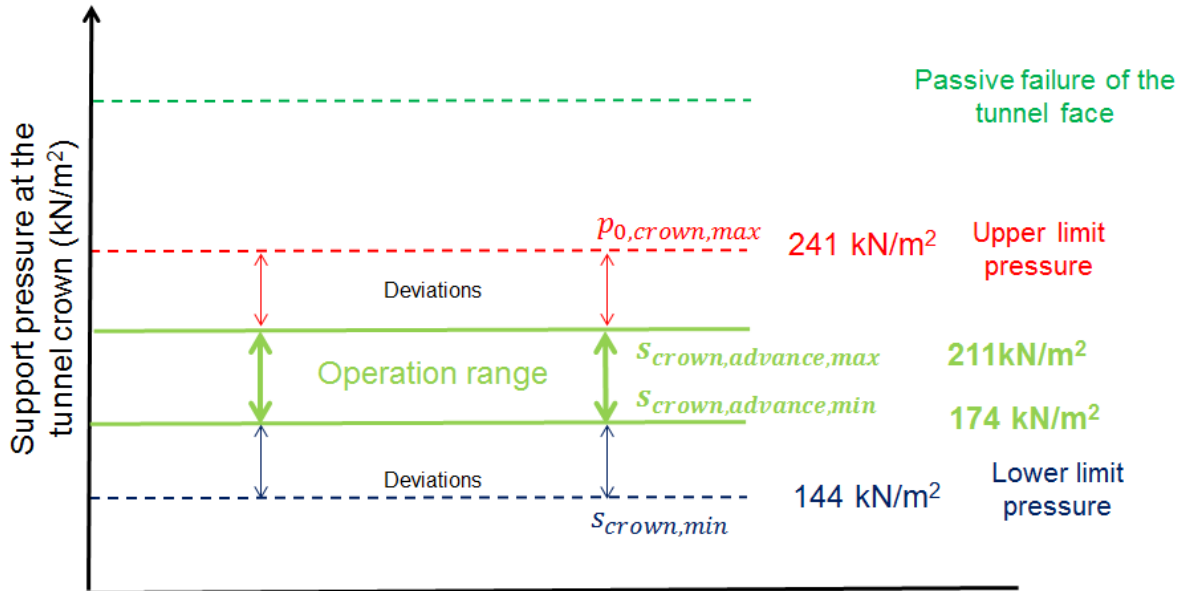


Fig. 33: Support pressure limits at the tunnel crown of Case 2 with excavation in clayey soils

## 9 References

### 9.1 General references

- [1] Abe T., Sugimoto Y., Ishihara K. (1978): Development and application of environmentally acceptable new soft ground tunneling method. In: Proc. Int. Symp. "Tunnelling Under Difficult Conditions", Tokyo, pp. 315-320
- [2] Anagnostou, G. (2012): The contribution of horizontal arching to tunnel face stability. *Geotechnik* 35 (2012), Heft 1, pp. 34-44
- [3] Anagnostou G. & Kovari, K. (1994), The Face stability in Slurry-shield-driven Tunnels. *Tunnelling and Underground Space Technology* No. 2 1994, pp. 165-174
- [4] Anagnostou G. & Kovari K. (1996): Face Stability Conditions with Earth-Pressure-Balanced Shields. *Tunnelling and Underground Space Technology* No. 2 1996, pp. 165-173
- [5] Atkinson J. H., Mair R. J. (1981): Soil mechanics aspects of soft ground tunnelling. *Ground Engineering* 1981; 14, pp. 20–28.
- [6] Atkinson J.H., Potts D.M. (1977): Stability of a shallow circular tunnel in cohesionless soil. *Géotechnique* 1977; 27: 203–15.
- [7] Berthoz N. et al. (2012): Face failure in homogeneous and stratified soft ground: Theoretical and experimental approaches on 1g EPBS reduced scale model. *Tunnelling and Underground Space Technology* 30 (2012), pp. 25–37
- [8] Bezuijen A., Messemaeckers-van de Graaf C. A. (1997): Stabiliteit van het graaffront bij vloeistofondersteuning. Technical Report 33, Boren Tunnels, en Leidingen, 1997
- [9] Bezuijen A. (2009): The influence of grout and bentonite slurry on the process of TBM tunnelling, *Geomechanics and Tunnelling* 2 (2009), No. 3, pp. 294-303, DOI: 10.1002/geot.200900025
- [10] Bezuijen A., Pruiksma J. P., van Meerten H. H. (2001): Pore pressures in front of tunnel, measurements, calculations and consequences for stability of tunnel face, In Adachi, T., K. Tateyama & M. Kimura (eds), *Modern Tunneling Science and Technology*, pp. 799–804. Rotterdam, Balkema
- [11] Bezuijen A., Schaminée P. E. L. (2001): Simulation of the EPB-shield TBM in model test with foam as additive, Proc. IS-Kyoto 2001 conference on Modern Tunneling Science and Technology, pp. 935 - 940
- [12] Broere W., van Tol A.F. (1998): Face stability calculation for a slurry shield in heterogeneous soft soils. Nego, Jr. & Ferreira (eds.) *Tunnels and Metropolises*, Sao Paolo, Brazil, 1998, pp. 215–218.
- [13] Broere W., van Tol A. F. (2000): Influence of infiltration and groundwater flow on tunnel face stability. In Kusakabe, O., K. Fujita & Y. Miyazaki (eds), *Geotechnical Aspects of Underground Construction in Soft Ground*, pp. 339-344. Balkema
- [14] Broere W. (2001): Tunnel face stability and new CPT applications. PhD thesis, Delft University
- [15] British Tunnelling Society in association with the Institution of Civil Engineers (2005): *Closed-Face Tunnelling Machines and Ground Stability - A guideline for best practice*, ISBN: 0 7277 3386 9
- [16] Broms B., Bennermark H. (1967): Stability of clay in vertical openings. *Journal of the Geotechnical Engineering Division, ASCE* 1967; 193: pp. 71–94.
- [17] Budach Ch. (2011): Beitrag zur Verwendung von Konditionierungsmitteln beim Einsatz von Erddruckschilden in grobkörnigen Lockergestein. Doctoral thesis, Ruhr-Universität Bochum (in German)
- [18] Budach, C.; Thewes, M. (2013): Erweiterte Einsatzbereiche von Erddruckschilden. *Geotechnik*. Volume 36, Heft 2, 2013, pp. 96-103, DOI: 10.1002/gete.201200012.

- [19] Budach C., Thewes M. (2015): Application ranges of EPB shields in coarse ground based on laboratory research, *Tunnelling and Underground Space Technology* 50 (2015) , pp. 296–304
- [20] Casarin C. and Mair R. J. (1981): The assessment of tunnel stability in clay by model tests. In: *Soft-Ground Tunnelling: Failures and Displacements*. A.A. Balkema, Rotterdam, Netherlands, pp. 33-44.
- [21] Chambon P. & Corte J. F. (1989): Stabilité du front de taille d'un tunnel faiblement enterré: modélisation en centrifugeuse. In *Proc. Int. Conf. Tunneling and Microtunneling in Soft Ground: From Field to Theory*, Paris, pp. 307 – 315 (In French)
- [22] Chambon P. & Corté J.F. (1994): Shallow Tunnels in Cohesionless Soil: Stability of Tunnel Face. *J. Geotech. Engineer.*, 120(7), pp. 1148–1165.
- [23] Chen R. et al. (2013): Experimental study on face instability of shield tunnel in sand. *Tunnelling and Underground Space Technology* 33 (2013), pp. 12–21
- [24] Code for construction and acceptance of shield tunneling method, issued by ministry of housing and urban-rural of the development of the people's republic of China, Mar. 2008 (In Chinese)
- [25] DAUB (2010): Empfehlungen zur Auswahl von Tunnelvortriebsmaschinen, Deutscher Ausschuss für unterirdisches Bauen e. V. (DAUB), published 2010 at [www.daub-ita.de](http://www.daub-ita.de), also published in *Taschenbuch Tunnelbau 2011*, VGE Verlag GmbH (in German), English version to be found in Maidl et al. (2013)
- [26] Davis E.H., Gunn M.J, Mair, R.J., Seneviratne H.N. (1980): The stability of shallow tunnels and underground openings in cohesive material. *Géotechnique* 30 (4), pp.397–416
- [27] DIN 4085:2007-10: Baugrund – Berechnung des Erddruckes (Subsoil – calculation of earth-pressure), 2007 (in German)
- [28] DIN 4126:2013-09: Nachweis der Standsicherheit von Schlitzwänden (Stability analysis of diaphragm walls), 2013 (in German)
- [29] Eurocode 7 - EN 1997: Geotechnical design (2006)
- [30] Galli M.; Thewes M. (2014): Investigations for the application of EPB shields in difficult grounds. *Untersuchungen für den Einsatz von Erddruckschilden in schwierigem Baugrund*. *Geomechanics and Tunnelling* 7, No. 1, 2014, pp. 31-44, DOI: 10.1002/geot.201310030.
- [31] Girmscheid G. (2008): *Baubetrieb und Bauverfahren im Tunnelbau*, Ernst und Sohn Verlag, Berlin (in German)
- [32] Hollmann F.; Thewes M. (2013): Assessment method for clay clogging and desintegration of fines in mechanised tunnelling. *Tunnelling and Underground Space Technology* Vol. 37, 2013, pp. 96-106, DOI: 10.1016/j.tust.2013.03.010.
- [33] Holzhäuser J., Hunt S. W., Mayer C. (2006): *Global experience with soft ground and weak rock tunneling under very high groundwater heads*, North American Tunneling Chicago, IL., Taylor & Francis Group London, ISBN 0 415 40128 3
- [34] Horn, N. (1961): Horizontaler Erddruck auf senkrechte Abschlussflächen von Tunnelröhren. In *Landeskonferenz der Ungarischen Tiefbauindustrie*, pp. 7–16 (in German).
- [35] Hu, X., Zhang, Z., Kieffer S. (2012): A real-life stability model for a large shield-driven tunnel in heterogeneous soft soils, *Front. Struct. Civ. Eng.* 2012, 6(2), pp. 176-187
- [36] Japan Society of Civil Engineers: *Standard specifications for tunnelling – 2006: Shield Tunnels*
- [37] Jancsecz S., Steiner W. (1994): Face support for a large mix-shield in heterogeneous ground conditions, in *Proc Tunnelling '94*, pp. 531-550, Chapman and Hall, London
- [38] Janssen H. A. (1895) *Versuche über Getreidedruck in Silozellen*. *Zeitschrift des Vereins deutscher Ingenieure*, Band XXXIX, No. 35, pp. 1045-1049 (in German)

- [39] Kanayasu S., Kubota I., Shikubu N. (1995): Stability of face during shield tunnelling – A survey on Japanese shield tunnelling. in *Underground Construction in Soft Ground* (eds. K. Fujita and O. Kusakabe), pp. 337-343, Balkema, Rotterdam
- [40] Kirsch A. (2009): On the face stability of shallow tunnels in sand, No. 16 in *Advances in Geotechnical Engineering and tunnelling*. PhD Thesis, University of Innsbruck, Logos, Berlin
- [41] Kirsch A. (2010): Numerical investigation of the face stability of shallow tunnels in sand. *Numerical Methods in Geotechnical Engineering*, Benz & Nordal (eds), Taylor & Francis Group, London, pp. 779-784
- [42] Kirsch A., Kolymbas D. (2005): Theoretische Untersuchung zur Ortsbruststabilität. *Bautechnik* 82(7): pp. 449–456
- [43] Kimura T., Mair R.J. (1981): Centrifugal testing of model tunnels in soft clay. In: *Proceedings of 10 th International Conference on Soil Mechanics and Foundation Engineering*, Stockholm, 15 –19 June 1981. Rotterdam: Balkema, pp. 319–22.
- [44] Leca E. & Dormieux L. (1990): Upper and lower bound solutions for the face stability of shallow circular tunnels in frictional material. *Géotechnique*, Vol. 40, no 4, pp. 581-605
- [45] Leca E., New B.: (2007): ITA/Aites report: Settlements induced by tunneling in Soft Ground. *Tunnelling and Underground Space Technology* 22, pp. 119-149
- [46] Li Y., Emeriault F., Kastner R., Zhang Z. X. (2009): Stability of large slurry shield-driven tunnel in soft clay, *Tunnel and Underground Space Technology* 24, pp. 472-481
- [47] Longchamp P. (2005): AFTES recommendations concerning slurry for use in slurry shield TBM, *Tunnels et ouvrages souterrains*, No. 1 2005, S. 164-183
- [48] Maidl B., Herrenknecht M., Maidl U., Wehrmeyer G. (2013): *Mechanised Shield Tunnelling*, Ernst und Sohn Verlag, Berlin
- [49] Maidl, U. (1995): Erweiterung der Einsatzbereiche der Erddruckschilde durch Bodenconditionierung mit Schaum, Doctoral thesis, Ruhr-Universität Bochum (in German)
- [50] Mair, R.J. (1979): Centrifugal modelling of tunnel construction in soft clay. PhD thesis, University of Cambridge
- [51] Mayer P.M., Hartwig U., Schwab C. (2003): Standsicherheitsuntersuchungen der Ortsbrust mittels Bruchkörpermodell und FEM, *Bautechnik* 80, pp. 452-467 (in German)
- [52] Mélix P. (1987): Modellversuche und Berechnungen zur Standsicherheit oberflächennaher Tunnel. *Veröff. des Inst. für Boden- und Felsmechanik der Univ. Fridericiana in Karlsruhe*, 103 (1987) (in German)
- [53] Merritt A. S., Mair, R. J. (2008): Mechanics of tunnelling machine screw conveyors: a theoretical model. *Geotechnique* 58, No. 2, pp. 79–94, doi: 10.1680/geot.2008.58.2.79
- [54] Messerli J., Pimentel E., Anagnostou G. (2010): Experimental study into tunnel face collapse in sand. In: *Springman, Laue, Seward (Eds.), Physical Modelling in Geotechnics*, vol. 1, pp. 575–580.
- [55] Mohkam M., Wong Y. W. (1989): Three dimensional stability analysis of the tunnel face under fluid pressure. In G. Swoboda, editor, *Numerical Methods in Geomechanics*, pp 2271–2278, Rotterdam, 1989. Balkema
- [56] Mollon G., Dias D., Soubra A.H. (2010): Face stability analysis of circular tunnels driven by a pressurized shield. *J.Geotech. Geoenviron. Eng.* 2010; 136: pp 215–29.
- [57] Mollon G., Dias D., Soubra A. H. (2011): Rotational failure mechanisms for the face stability analysis of tunnels driven by a pressurized shield. *Int. J. Numer. Anal. Methods Geomech*; 35, pp. 1363–88.
- [58] Mueller-Kirchenbauer, H. (1977): Stability of slurry trenches in inhomogeneous subsoil. *Proceedings of 9th International Conference on Soil Mechanics and Foundation Engineering*, Vol. 2, Tokyo.

- [59] NTC - "Norme Tecniche per le Costruzioni" - Italian design code (2014), last revision issued by Ministry of Infrastructures and Transport and approved by CSLPP on October 2014 (not in force yet), (in Italian)
- [60] ÖGG - Österreichische Gesellschaft für Geomechanik (2012): Richtlinie für die geotechnische Planung von Untertagebauten mit kontinuierlichem Vortrieb – Entwurf 2012. ÖGG 2012, Salzburg (in German)
- [61] Piaskowski A., Kowalewski Z. (1965): Application of thixotropic clay suspensions for stability of vertical sides of deep trenches without strutting, Proc. Of 6<sup>th</sup> Int. Conf. on Soil Mech. And Found. Eng. Montreal, Vol. 111
- [62] Plekkenpol J. W., van der Schrier J. S., Hergarden H. J. A. M. (2005): Shield tunnelling in saturated sand - face support pressure and soil deformations, Tunnelling. A Decade of Progress. GeoDelft 1995-2005
- [63] Peck, R. B. (1969): Deep excavation and tunnelling in soft ground. State of the Art Report. Proceedings of the 7th ICSMFE, Mexico, pp.255-284
- [64] Peila D., Oggeri C., Vinai C. (2007): Screw conveyor device for laboratory tests on conditioned soil for EPB tunneling operations, Journal of Geotechnical and Geoenvironmental Engineering, 2007, pp. 1622 – 1625
- [65] Quebaud S., Sibai M., Henry J.-P. (1998): Use of Chemical Foam for Improvements in Drilling by Earth-Pressure Balanced Shields in Granular Soils. Tunnelling and Underground Space Technology, Vol. 13, No. 2, pp. 173-180
- [66] Richtlinie 853 (RIL)- Eisenbahntunnel planen, bauen und instand halten, Aktualisierung 2013, Deutsche Bahn AG (in German)
- [67] Senent et al. (2013): Tunnel face stability in heavily fractured rock masses that follow the Hoek–Brown failure criterion. International Journal of Rock Mechanics & Mining Sciences 60, pp. 440–451
- [68] Thewes M. (2007): TBM tunneling challenges – redefining the state of the art, Key-note Lecture ITA – AITES WTC 2007 Prague, Tunnel, pp. 13 - 27
- [69] Thewes, M. (2009): Bentonite slurry shield machines In: de Pérez Ágreda, Eduardo Alonso; de Álvarez Toledo, Marcos Arroyo (Eds.): Operación y mantenimiento de escudos: presente y futuro. Barcelona, Universitat politècnica de Catalunya, 2009, pp. 41-68
- [70] Thewes, M. (2010): Shield tunnelling technology for increasingly difficult site conditions In: Zlámál; Butovič; Hilar (Eds.): Transport and City Tunnels: proceedings of the 11th international conference underground constructions Prague 2010. Prague: Czech Tunneling Association ITA-AITES, 2010, pp. 371-379
- [71] Thewes M.; Budach C. (2010): Soil Conditioning with Foam during EPB-Tunnelling (Konditionierung von Lockergesteinen bei Erddruckschilden). Geomechanics and Tunnelling, Vol. 3, No. 3, 2010, pp. 256-267.
- [72] Thewes M., Budach C., Galli M. (2010): Laboruntersuchungen von verschiedenen konditionierten Lockergesteinsböden für Tunnelvortriebe mit Erddruckschildmaschinen, Tunnel, Nr. 6, pp. 21 - 30
- [73] Thewes, M. (2004): Schildvortrieb mit Flüssigkeits- oder Erddruckstützung in Bereichen mit gemischter Ortsbrust aus Fels und Lockergestein. Geotechnik 27, 2004/2, pp. 214-219.
- [74] Triantafyllidis T. (2004): Planung und Bauausführung im Spezialtiefbau, Teil 1: Schlitzwand- und Dichtwandtechnik, Ernst & Sohn Verlag, Berlin (in German)
- [75] Terzaghi K. & Jelinek R. (1954): Theoretische Bodenmechanik, Springer-Verlag, Berlin (in German)

- [76] U.S. Department of Transportation, Federal Highway Administration (2009): Technical Manual for Design and Construction of Road Tunnels —Civil Elements – general statements about the necessity of the tunnel stability investigation.
- [77] Vermeer P., Ruse N., Marcher T. (2002): Tunnel heading stability in drained ground, Felsbau, 20 No. 6, pp. 8 – 19
- [78] Vinai R. (2006): A contribution to the study of soil conditioning techniques for EPB TBM applications in cohesionless soils, Ph.D. thesis, Politecnico di Torino, Italy, 2006
- [79] Vu M. N., Broere W., Bosch J. (2015): The impact of shallow cover on stability when tunnelling in soft soils, Tunnelling and Underground Space Technology 50, pp. 507 - 515
- [80] Walz, B., J. Gerlach & M. Pulsfort (1983): Schlitzwandbauweise, Konstruktion, Berechnung und Ausführung. Technical Report, Bergische Universität Gesamthochschule Wuppertal. (in German)
- [81] Yu H. A., Salgado R., Sloan S. W., Kim J. M. (1998): Limit analysis versus Limit equilibrium for slope stability, Journal of Geotechnical and Geomechanical engineering, January 1998, pp. 1-11
- [82] Zusätzliche Technische Vertragsbedingungen und Richtlinien für Ingenieurbauten (short form ZTV-ING) – Teil 5 Tunnelbau (2012), Bundesanstalt für Strassenwesen (in German)
- [83] Zizka Z., Schoesser B., Thewes M. (2013): Face Stability Assessment of Large-diameter Slurry Shields. Proceedings of the Third International Conference on Computational Methods in Tunnelling and Subsurface Engineering, Ruhr-University Bochum, April 17-19, 2013, Aedificatio Publishers, Freiburg, 2013, pp. 663-674.
- [84] Zhang Z.X, Hu X. Y., Kieffer D. S. (2011): A discrete numerical approach for modeling face stability in slurry shield tunnelling in soft soils. Computers and Geotechnics 38, pp. 94–104

## 9.2 Websites references

- [85] [www.herrenknecht.de](http://www.herrenknecht.de)
- [86] <http://www.daub-ita.de/start/>